Since January 2020 Elsevier has created a COVID-19 resource centre with free information in English and Mandarin on the novel coronavirus COVID-19. The COVID-19 resource centre is hosted on Elsevier Connect, the company's public news and information website.

Elsevier hereby grants permission to make all its COVID-19-related research that is available on the COVID-19 resource centre - including this research content - immediately available in PubMed Central and other publicly funded repositories, such as the WHO COVID database with rights for unrestricted research re-use and analyses in any form or by any means with acknowledgement of the original source. These permissions are granted for free by Elsevier for as long as the COVID-19 resource centre remains active.

Photodiagnosis and Photodynamic Therapy 34 (2021) 102221

Contents lists available at ScienceDirect

Photodiagnosis and Photodynamic Therapy

journal homepage: www.elsevier.com/locate/pdpdt

A systematic review of photodynamic therapy as an antiviral treatment: Potential guidance for dealing with SARS-CoV-2

Pollyanna C.V. Conrado [a], Karina M. Sakita [a], Glaucia S. Arita [a], Camila B. Galinari [a], Renato S. Gonçalves [b], Luciana D.G. Lopes [a], Maria V.C. Lonardoni [a], Jorge J.V. Teixeira [a], Patrícia S. Bonfim-Mendonça [a], Erika S. Kioshima [a,*]

[a] Department of Analysis Clinics and Biomedicine, State University of Maringa, Parana, Brazil
[b] Department of Chemistry, State University of Maringa, Parana, Brazil

ARTICLE INFO

Keywords:
Photodynamic therapy
Photosensitizers
Photoinactivation
Viruses
SARS-CoV-2

ABSTRACT

Background: SARS-CoV-2, which causes the coronavirus disease (COVID-19), presents high rates of morbidity and mortality around the world. The search to eliminate SARS-CoV-2 is ongoing and urgent. This systematic review seeks to assess whether photodynamic therapy (PDT) could be effective in SARS-CoV-2 inactivation.
Methods: The focus question was: Can photodynamic therapy be used as potential guidance for dealing with SARS-CoV-2?". A literature search, according to PRISMA statements, was conducted in the electronic databases PubMed, EMBASE, SCOPUS, Web of Science, LILACS, and Google Scholar. Studies published from January 2004 to June 2020 were analyzed. *In vitro* and *in vivo* studies were included that evaluated the effect of PDT mediated by several photosensitizers on RNA and DNA enveloped and non-enveloped viruses.
Results: From 27 selected manuscripts, 26 publications used *in vitro* studies, 24 were exclusively *in vitro*, and two had *in vitro/in vivo* parts. Only one analyzed publication was exclusively *in vivo*. Meta-analysis studies were unfeasible due to heterogeneity of the data. The risk of bias was analyzed in all studies.
Conclusion: The *in vitro* and *in vivo* studies selected in this systematic review indicated that PDT is capable of photoinactivating enveloped and non-enveloped DNA and RNA viruses, suggesting that PDT can potentially photoinactivate SARS-CoV-2.

1. Introduction

The recent century has the biggest pandemic, a new disease that is affecting humanity lives, promoting high morbidity and mortality rates [1]. The first case was reported in late 2019, in Wuhan, Hubei Province (China). Since then, it has been spreading around the world [2]. Coronavirus disease-2019 (COVID-19) is caused by a novel coronavirus, formally named as SARS-CoV-2. This virus belongs to the family *Coronaviridae*, which may cause Severe Acute Respiratory Syndrome (SARS) in humans, similar to SARS-CoV and MERS-CoV [3,4].

SARS-CoV-2 is an enveloped β-coronavirus with a positive-sense, single-stranded RNA (ssRNA) genome of ~32 kb. The virion structure is constituted by spike (S) glycoprotein, envelope (E), membrane (M) and nucleocapsid (N) proteins [5,6]. The S protein of coronaviruses facilitates viral entry into target cells, by engaging to angiotensin-converting enzyme 2 (ACE2) receptor [7,8]. This receptor is located on the surface of cells, found mainly in the respiratory and gastrointestinal tract. The membrane fusion of virus with ACE2 receptor releases the viral genome into the host cytoplasm leading to viral replication, maturation, and virus release to infect other cells [6]. Besides that, SARS-CoV-2 include non-structural proteins known the open reading frames (ORFs), such as ORF1ab, ORF3a, ORF6, ORF7a, ORF10 and ORF8 that are involved in viral RNA replication and transcription, which are associated with the pathogenicity of virus and inhibited cellular immune responses [9,10].

Individuals infected with SARS-CoV-2 usually develop as main symptoms fever above 38 °C, dry cough, fatigue, dyspnea and difficulty breathing, which can range from asymptomatic infection to an acute highly contagious respiratory illness [11]. It is suggested that viral replication first occurs in the epithelium of the mucosa of the upper

* Corresponding author at: Division of Medical Mycology, Teaching and Research Laboratory in Clinical Analysis, Department of Clinical Analysis and Biomedicine of State University of Maringá, Av. Colombo, 5790, CEP: 87020-900, Maringá, Parana, Brazil.
E-mail address: eskcotica@uem.br (E.S. Kioshima).

https://doi.org/10.1016/j.pdpdt.2021.102221
Received 18 December 2020; Received in revised form 2 February 2021; Accepted 8 February 2021
Available online 15 February 2021
1572-1000/© 2021 Elsevier B.V. All rights reserved.

respiratory tract (nasal cavity and pharynx), multiplying in the lower respiratory tract and possibly the gastrointestinal mucosa [12].

Despite the collaborative efforts of researchers from all over the world, and the increase in publications in record time, only three therapeutic options were approved to combat the COVID-19 pandemic by the Food and Drug Administration. Therefore, the search for therapeutic options to control COVID-19 or to eliminate the new coronavirus is an urgent demand, given the capacity to widespread this pandemic and its number of deaths already achieved. Photodynamic therapy (PDT) has proven to be a promising alternative approach for photoinactivation of pathogenic microorganisms, such as fungus [13–15], bacteria [16,17], parasites [18,19], even in diseases caused by viruses in humans [20–22]. Besides that, the low cost, and non-toxicity of PDT shows satisfactory clinicals therapeutic results [23–26], including in immunocompromised individuals [27–29].

PDT is a non-invasive treatment, which requires the combination of a photosensitizer (PS), oxygen and a specific wavelength light irradiation, triggering photochemical reactions. Once the PS is light-activated in oxygen presence, it leads to reactive oxygen species (ROS) generation, causing irreversible damage in target structures, such as proteins and lipids, leading to the death of microorganisms by necrosis or apoptosis [30]. For viruses, PDT can affect lipid or protein membrane structures of the viral envelope, even nucleic acid, regardless of the specific interaction with a receptor, proving to be an efficient tool to eliminate these infectious agents [31–33]. In view of this, the PDT could be a therapeutic option for COVID-19, thus, this systematic review aims to assess whether photodynamic therapy and its mechanisms of action could be effective in inactivating SARS-CoV-2.

2. Materials and methods

The methodology rigor was defined in accordance to PRISMA guidelines (Preferred Reporting of Systematic Reviews and Meta-Analysis), which the focused question of review was “Could the photodynamic therapy have an effect on COVID-19?”. The flow diagram was used as strategy design on this study.

2.1. Literature research

A systematic review was conducted using PubMed, EMBASE, SCOPUS, Web of Science, Lilacs (Literatura Latino Americana em Ciências da Saúde) databases, and Google scholar in the period from 1 January, 2004, to the 30 June, 2020. Literature searches were conducted and screened to four independent research (PCVC, KMS, GSA and CBG). The first stage established an investigation to define the number of MeSH (Medical Subject Headings) terms in order to ensure high sensitivity and precision, and the researchers screened titles and abstract publications. Posteriorly, two experts (LDG and JJVT) validated the MeSH terms and Keywords strategy. For EMBASE, the research was divided in Group 1: “Virus” OR “RNA Viruses” OR “Middle East Respiratory Syndrome Coronavirus” OR “sars coronavirus” OR “Severe acute respiratory syndrome coronavirus 2”, AND Group 2 “Reactive Oxygen metabolite” OR “Photochemotherapy” OR “Photochemistry” AND Group 3 “Photosensitizing and Agents OR Virus and Inactivation”. Then, MeSH terms were organized on three groups for Pubmed research Group 1: “Viruses” OR “RNA Viruses” OR “Middle East Respiratory Syndrome Coronavirus” OR “SARS Virus” OR “severe acute respiratory syndrome coronavirus 2 [Supplementary Concept]”, AND Group 2: “Reactive Oxygen Species” OR “Photochemotherapy” OR “Photochemistry” AND Group 3: “Photosensitizing Agents” OR “Virus Inactivation”. SCOPUS free terms were to Group 1: Virus OR “RNA Viruses” OR “Middle East Respiratory” OR “Syndrome Coronavirus” OR “sars coronavirus” OR “Severe acute respiratory syndrome coronavirus AND 2”, Group 2: “Reactive Oxygen metabolite” OR Photochemotherapy OR Photochemistry, AND Group 3: “Photosensitizing Agents” OR “Virus inactivation”. For Web of Science, the same terms were used, but in the title (Ti) and topic term (TS) search. The research in Google scholar and LILACS used the descriptors by topic, following the same structure as the three groups of PubMed. The terms have been changed in the base Embase to ensure sensitivity and specificity.

2.2. Eligibility criteria

Articles that describe PDT as monotherapy, associated virus inactivation based on the titles and abstract were included in this review. Original articles in English from the defined period (2004–2020) with an abstract available in the database were evaluated and validated belong to the criteria of inclusion. Literature reviews, case reports, comments to the editor, letters, book chapters, patents, guidelines, pre-print and interviews were included to the exclusion criteria. Combination therapy, concerning the sequential or simultaneous use of PDT with conventional drugs such as antivirals and antibiotics in different experimental conditions were also included in the exclusion criteria due to in these approaches, a synergistic effect of the photosensitizer and the chemotherapy occurs at the therapeutic targets by different biochemical pathways, increasing the chances of viral inactivation.

2.3. Selection and quality assessment of relevant studies

The papers selected in the first stage, the full texts were retrieved in PDF format, numbered and randomly distributed among the four researchers from second stage to eligibility criteria. A consensus meeting was held to discuss disagreement after publications quality assessment. The references list were manually checked to recover publications that were not previously retrieved in the database research, to increase the review sensitivity and quality. Then, in the third stage, the selected papers were randomly distributed to four independent evaluators (ESK, PSBM, LDG and RSG), to ensure the validation of the selected papers by the researchers.

2.4. Data extraction

The fourth stage was composed of the four initial researchers (PCVC, KMS, GSA and CBG) with the support of two specialists (LDG, and JJVT) for topic structure. The articles were randomly distributed among the researchers for relevant data collection. By means of a table, important data were selected, including the following topics: reference, country, type of study *in vitro* (cell used or plasma), or *in vivo* (animal used), lineage of the virus, photosensitizer (PS), light source, wavelength, density/power, treatment protocol, results obtained and conclusion. Subsequently, the evaluators verified these data. Any discrepancies were resolved by consensus.

2.5. Risk of bias assessment

The quality and risk of bias in the selected papers were performed independently by four researcher specialists (JJVT, ESK, PBSM and LDG) based on the CONSORT (Consolidated Standards of Reporting Trials) guidelines [34]. For the analysis of 24 studies exclusively *in vitro*, we used a checklist composed of 15 domains. Among the 27 selected studies, only one was exclusively *in vivo* and used the Rob (Risk of Bias) tool for animal tests (Systematic Review Center for Laboratory Animal Experimentation - SYRCLE RoB tool). The ROB tool consists of 12 domains [35], described as a Cochrane adjusted risk model of the bias tool. The other two remaining studies presented mixed experiments (*in vivo* and *in vitro*). It is essential to report that, to date, no checklist allows the simultaneous analysis of two methods. In this sense, the checklists characterized above for verification separately for *in vivo* and *in vitro* studies were applied. The analysis of the quality of the bias of each publication was verified according to the scores from zero to ten for *in vivo* tests and from zero to 15 for *in vivo* tests. Checklists allow the quantification of scores, where high scores represent a low risk of bias;

low scores indicate a high risk of bias or "unclear" domains in publications.

3. Results

3.1. Literature search

Published studies were identified on six electronic databases. The literature search revealed a total of 469 records from the primary search and 13 additional relevant articles were found through references. After removal of 282 duplicates, the total 295 articles were scanned of which 33 full-text articles were assessed for eligibility criteria and 6 studies were excluded since these did not fulfill the inclusion criteria. Therefore, 27 studies were included in this review as shown in Fig. 1.

3.2. Heterogeneity of the analyzed variables

3.2.1. Photosensitizers

In the 26 *in vitro* articles included in this review as shown in Table 1, 39 different types of PS were identified, and six articles used more than one PS alternative [33,37,39,40,42,56]. In this context, there was a predominance of compounds derived from porphyrin represented 30.7 % (n = 12/39), with emphasis on compounds Protoprophyrin IX (PPIX); Zn-protoporphyrin IX (ZnPPIX); Mesoporphyrin IX (MPIX); Porphyrin derivative; Tetraphenylporphyrin (TPP); Neutral 1b and Cationic tri-pyridylporphyrin-D-galactose 3b; Cationic porphyrin, mono-phenyl-tri-(N-methyl-4-pyridyl)-porphyrin chloride [Tri-P(4)]; Meso-tetraphenylsulfonated porphyrins (TPPMS4); TPPFeS4; TPPMnS4; TPPPdS4; TPPZnS4 and Hematoporphyrin monomethyl ether (HMME) [40,45,48,54–56,59]. The phthalocyanines group represented 20.5 % (n = 8/39) of the PS, as Zinc tetracarboxy-phthalocyanines (ZnPc); Aluminum tetracarboxy-phthalocyanines (AlPc); Oligolysine-conjugated zinc(II) Phthalocyanines; Conjugate 1 Dilysine-Phthalocyanine; Conjugate 2 Tetralysine-Phthalocyanine; Octalysine-Phthalocyanine Conjugate 3; Octacationic octakis(cholinyl) zinc phthalocyanine (Zn-PcChol8+) and Zinc phthalocyanine (ZnPc) with upconversion nanoparticles (UCNs) – (ZnPc-UCNs)) [39,42,44,47]. Less frequently were the following PS naphthalene derivatives (Azido-naphthalene (AzNAP); 1,5-diazidonaphthalene (DAN); 1,5-Diiodonaph-thalene (DINAP), 7.6 % (n = 3/39) [37], oxazolidine (JL103, JL118, JL122), 7.6 % (n = 3/39) [33] and to Amotosalen derivatives (Amoto-salen−HCl and Amotosalen) 5 % (n = 2/39) [52,53] respectively. The following PS were not grouped, and individually correspond to 2.6 % (n = 1/39), such as 5-aminolevulinic acid (ALA) [36], Solid phase fullerene-based PS (SPFPS) [38], Ortoquin [32], Indocyanine green (ICG) [50], rhodanine derivative (LJ001) [33], Fotoditazine [60], Hypericin (Hy) [58], Diazidobiphenyl derivative (DABIPH) [37] and benzochlorine derivative (Zn-BC-AM) [43], Methylene blue (MB) [41, 49] and curcumin (CUR) [51,57]. Highlight MB and CUR which were the most frequent PS in analyzed articles.

Three *in vivo* articles (Table 2) were included, in which three different types PS were used, the majority are Phthalocyanine products; Phthalocyanine (Pc 4); Zinc phthalocyanine with upconversion nano-particles (ZnPc-UCNs), represented at a rate of 66.7 % (n = 2/3) [46,47] and CUR with 33.3 % (n = 1/3) [57].

3.2.2. Light sources

Thirteen different light source models were found in the 26 analyzed

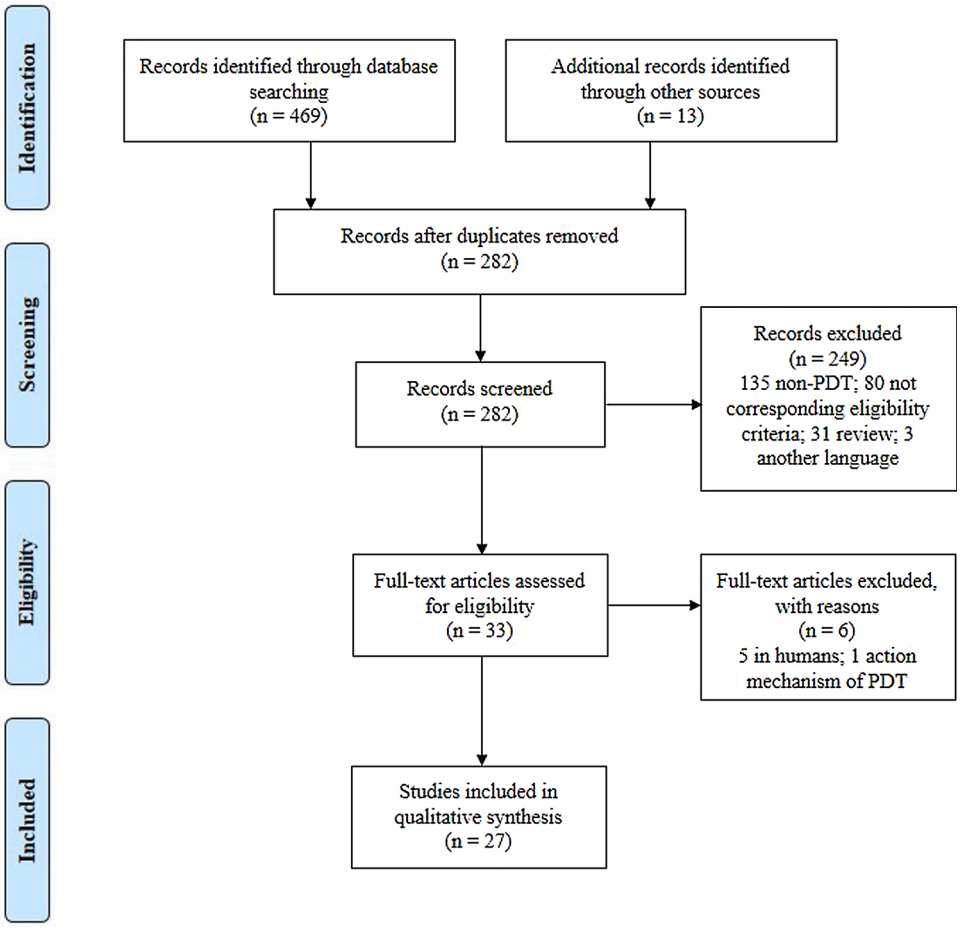

Fig. 1. Flow diagram of studies selected for the systematic review.

Table 1
In vitro studies of PDT on viruses from 2004 to 2020.

Author / Year	Country	Virus	Virus genome type (Virus group)	Cell/sample type	Photosensitizer (PS) Concentration used and time of exposure to PS	Light source / Wavelenght / Fluence / Pontence-density / Time of exposure / Iluminance	Protocol	Measurement of results	Main outcomes	Conclusion
Ayala, F., et al. 2008 [38]	Italy	Herpes simplex virus type 1 (HSV-1)	DNA (enveloped)	Immortal keratinocyte cell line (HaCat)	5-aminolaevulinic acid (ALA) 0.05 and 0.1 mM 3 h	Tungsten lamp 580 nm 18 J/cm^2 20 mW/cm^2 15 min or every 15 mins until 1 h completly –	HaCat cells line were seeded 1×10^6 cells/well and infected with HSV-1 virus at 5 PFU/cell in three moments: Preadsorption period: HaCat cells were treated with ALA-PDT, then infected with HSV-1 and incubated for 1 hour. Adsorption period: HaCat cells were treated with ALA, infected with virus during 1 hour and photoirradiated every 15 min until complete 1 h. Post-adsorption period: HaCat cells were infected with virus and incubated for 1 hour, then ALA-PDT.	Supernatants from infected cells were harvested at 24 and 48 h and tested for their ability to form plaques in the HaCat cells using a standard titration method by crystal violet.	Post-adsorption assay treatment with ALA-PDT has a concentration-dependent inhibition of HSV-1 replication, about 40 % for ALA at 0.05 mM and about 70 % for ALA at 0.1 mM.	ALA–PDT acts directly on HSV-1 in a late phase of the viral cycle and, therefore, on neoformate viral particles, causing damage that limits the spread of the virus from cell to cell.
Belanger, J. M., et al. 2010 [39]	United States of America	Human immunodeficiency virus (HIV-1)	RNA (enveloped)	TZM-bl cells	1-Azidonaphthalene (AzNAP) 1,5-diazidonaphthalene (DAN) 4,4′-diazidobiphenyl (DABIPH) 1,5-Diiodonaphthalene (DINAP) 100 μM 5 min	UVA light 335 nm – 10 mW/cm^2 2 min –	Cells were seeded at 2×10^4 cells/well and added photoinactivated HIV-1 3.1×10^3 ng/mL of total protein per well.	Luciferase activity was analyzed after 18–24 h, using the Steady-Glo Luciferase System (Promega) and using infectious controls of the same viral lot in serial dilution.	All azido-based compounds-PDT reduced aproximatelly 90000 luminescence units at 100 μM, causing a total viral photoinactivation.	Azido-containing hydrophobic compounds based on naphthalenic or biphenyl structures can be used to rapidly and efficiently inactivate HIV-1 when irradiated by UVA light with short irradiation times.
Belousova, I. M., et al. 2014 [40]	Russia	Influenza virus A/ Puerto Rico/8/34 (H1N1)	RNA (enveloped)	Madin–Darby canine kidney cells (MDCK)	Solid phase fullerene-based PS (SPFPS) 0.2, 0.5, 2.0 g/mL –	Double-sided panel of Edison diodes 460 nm 0−648 J/cm^2 160−200 mW/cm^2 10 min	The concentrations of SPFPS were added to virus-containing albumin solution 7.0-9.5 $\log_{10}EID_{50}$/0.2 mL H1N1. After photoinactivation,	Infectious titer of the virus was determined as decimal logarithm of reciprocal to the maximal dilution of the specimen causing positive hemagglutination reaction after 48 h.	The decrease of infectious activity of the virus reached 7.0–8.5 orders. For effective inactivation the dose of irradiation should not be lower than	The SPFPS-PDT can be a procedure of inactivation of viruses in the preparations of the plasma of donor blood.

(*continued on next page*)

Table 1 (*continued*)

Author / Year	Country	Virus	Virus genome type (Virus group)	Cell/sample type	Photosensitizer (PS) Concentration used and time of exposure to PS	Light source / Wavelenght / Fluence / Pontence-density / Time of exposure / Iluminance	Protocol	Measurement of results	Main outcomes	Conclusion
					–	–	supernatant was removed for virus infectious activity evalution on MDCK cells.		324 J/cm^2 and concentration of SPFPS should be 0.2 g/ml or higher.	
Cocca, L. H. Z., et al. 2017 [41]	Brazil	Bovine herpesvirus type 1 (BoHV-1)	DNA (enveloped)	Madin-Darby bovine kidney cells (MDBK)	Zinc (ZnPc) Aluminum tetracarboxy-phthalocyanines (AlPc) 5 and 10 μM 1 h	Halogen lamp – – 180 mW/cm^2 15, 30, 45 or 60 min –	Viral suspension containing $10^{5.75}$ $TCID_{50}$/mL was incubated with the PSs and incubated in the dark, and irradiated in differents time of 15 to 60 min. After photoinactivation, the suspension were inoculated into the MDBK cells	After 72 h, the viability of the virus was evaluated by titration and the cells cytopathic effect was determined using an inverted microscope.	BoHV-1 was completely photoinactived by both PS (ZnPc and AlPc) with an irradiation for 60 min. However, ZnPc (10 μM) was able to reduce 4 logs in viral titer after 15 min of irradiation. The complete inactivation was observed after 30 min. No changes in cell morphology was observed.	ZcPc and AlPc mediated PDT are promising for photoinactivation of BoHV-1
Cruz-Oliveira, C., et al. 2017 [42]	Brazil Portugal	Vesicular stomatitis virus (VSV)	RNA (envoloped)	Baby hamster kidney cell (BHK-21)	Protoprophyrin IX (PPIX) Zn-protoporphyrin IX (ZnPPIX) Mesoporphyrin IX (MPIX) 0.001, 0.01 or 0.1 μM –	Fluorescent lamp – – 30 W – 2.000 lx	Concentrations of each PS were added directly to the cell culture, VSV infection was carried out with nonpurified virus at an MOI of 1, and illuminated.	At 6 h postinfection of virus and photoinactivaton, the viability was determined as PFU and IC_{50} for BHK-21 cells.	Photoactivation with 0.1 μM of ZnPPIX, 0.1 μM of MPIX or 0.01 μM PPIX show a reduction of approximately 8 log_{10}, 6.5 log_{10} and 5 log_{10} respectively to each PS and completely abolished VSV infectivity.	The PPIX, ZnPPIX, and MPIX mediated by PDT has antiviral activity against VSV.
Huang, Q., et al. 2004 [43]	China	Dengue virus (DENV)	RNA (enveloped)	African green monkey kidney cell line (Vero)	Methylene blue (MB) 0.1, 0.5, 1.0 or 2.0 μg/mL –	LED red light 664 nm – – 5, 10, 15, 20 or 25 min 5.000 mlx	2×10^6 PFU/mL DENV was mixed with each PS concentration and irradiated by different times and distances. After, the virus suspensions photoinativated were incubated with Vero cells for 6–8 days.	After 6–8 days PFU assay was performed, and KLV ($lgN_0 = lgN_\times$) was determined.	DENV was completely inactivated (≈ 6.30 virus titer / 2×10^6 PFU) from ≥1.0 μg/mL MB-PDT at distance 2.5 meters irratiated 5 min, and to distance of 3.0 m, at 2.0 μg/mL and irradiated for 20 min.	MB working concentration and illumination intensity, time and distance are the four key factors affecting the inactivation efficiency of the MB/narrow bandwidth light system. However, it was effective disinfectant tool for

(*continued on next page*)

Table 1 (*continued*)

Author / Year	Country	Virus	Virus genome type (Virus group)	Cell/sample type	Photosensitizer (PS) Concentration used and time of exposure to PS	Light source / Wavelenght / Fluence / Pontence-density / Time of exposure / Iluminance	Protocol	Measurement of results	Main outcomes	Conclusion
										inactivating enveloped RNA.
Ke, M.-R., et al. 2014 [44]	China	Influenza A virus (H1N1) Herpes simplex virus type 1 (HSV1) Adenovirus type 3 (Ad3) Coxsackievirus (Cox B1)	RNA (enveloped) DNA (enveloped) DNA (non-enveloped) RNA (non-enveloped)	Human larynx epidermoid carcinoma cells (HEp-2) Madin–Darby canine kidney cells (MDCK)	Oligolysine-conjugated zinc(II) Phthalocyanines Conjugate 1 Dilysine-Phthalocyanine Conjugate 2 Tetralysine-Phthalocyanine Conjugate 3 Octalysine-Phthalocyanine Up to 8 μM 1 h	Halogen lamp 610 nm 48 J/cm^2 40 mW/cm^2 20 min –	100 $TCID_{50}$ of the corresponding viruses was incubated with various concentrations of phthalocyanine solutions in the dark, and irradiated. After photoinactivation, the viral samples were inoculated into the cells HEp-2 or MDCK with 70–80% confluence, and incubated.	After 72 h, the cytopathic effect was determined by IC_{50}, that was used to construct a dose-response curve.	Conjugates 1, 2 and 3 showed inibhition against the enveloped viruses at IC_{50} concentrations 0.17, 0.11 and 0.05 nM respectively,for H1N1, and 0.46, 0.79 and 0.05 nM for HSV1. These compounds did not have effect against the nonenveloped viruses Ad3 and Cox B1.	The Oligolysine-conjugated zinc(II) Phtalocyanines compounds are promising for the photoinactivation of enveloped viruses.
Koon, H.-K., et al. 2010 [45]	China	Epstein-Barr virus (EBV)	DNA (enveloped)	HK-1 cells	Zn-BC-AM 2 μM 24 h	Tungsten lamp 682 ± 5 nm 0.25, 0.5 or 1.0 J/cm^2 0.8 mW/cm^2 – –	Zn-BC-AM was added on HK-1-EBV cells infected virus at 4.5×10^5 cells/mL, incubated in the dark, and irradiated and reincubated.	After 24 h post-Zn-BC-AM-PDT, the cells were analyzed by flow cytometry with propidium iodide (PI) and excitation wavelength at 488 nm.	Zn-BC-AM-PDT induced the death of HK-1-EBV in 50 % with irradiation dose at 0.5 J/cm^2 and 80% at 1 J/cm^2.	The photoinactivation with Zn-BC-AM showed activity against HK-1 cells infected with EBV.
Korneev, D., et al 2019 [46]	Australia Russia	Avian influenza A virus (H5N8)	RNA (envoloped)	Madin-Darby canine kidney (MDCK) cells	Octacationic octakis (cholinyl) zinc phthalocyanine (Zn-PcChol8+) 2 and 4 μM –	Halogen lamp – 12 J/cm^2 10 mW/cm^2 20 min –	MDCK cells were grown to 90 % confluency and infected with 10-fold serial dilutions (from 10^{-1} to 10^{-8}) of H5N8 virus photoinactivated with concentrations Zn-PcChol8+, and reincubated.	After 5 days, the virus-induced cytopathic effect was detected and virus titers were determined by $TCID_{50}$.	The cytopathic effect of cells infected with H5N8 photoinactivated with Zn-PcChol8+ showed complete inactivation for both concentrations.	The PDT mediated by Zn-PcChol8+ was able to inactivate the influenza virus and detach the influenza virus surface glycoproteins, promoting the loss of infectivity as visualized on TEM.
Latief, M. A., et al. 2015 [47]	Japan Indonesia	Acyclovir (ACV)-resistant HSV-1 Herpes simplex virus type 1 (HSV-1)	DNA (enveloped) DNA (enveloped)	Human FL cell line	Porphyrin derivative TONS 504 0.01, 0.1, 0.5, 1.0 and 10 mg/L 5 min	LED 660 nm 10, 20 or 30 J/cm^2 0.55 W 3 min, twice 3 min or three times 3 min –	Confluents human FL cells were infected with the viral strains ACV and HSV-1 at 0.02 MOI for 1 hour, supernatant was removed and reincubated for more 3 h. Then, concentrations of PS	After 24 h of photoinactivation, immunocytofluorescence analysis with rabbit antibodies to HSV-1 was performed.	Complete eradication of both viruses was apparent at a TONS 504 concentration of 10 mg/l and light energy of 10 to 30 J/cm^2 as well as at a TONS 504 concentration of 1 mg/l and light	The novel porphyrin derivative TONS 504 mediated by PDT showed a deleterious effect on host cells infected with HSV-1 and ACV.

(*continued on next page*)

Table 1 (*continued*)

Author / Year	Country	Virus	Virus genome type (Virus group)	Cell/sample type	Photosensitizer (PS) Concentration used and time of exposure to PS	Light source / Wavelenght / Fluence / Pontence-density / Time of exposure / Iluminance	Protocol	Measurement of results	Main outcomes	Conclusion
							were added, incubated in the dark, irradiated, and reincubated.		energy of 20 or 30 J/cm^2.	
Lim, M. E., et al. 2012 [49]	Singapore	Dengue virus serotype 2 (DENV 2)	RNA (enveloped)	Human hepatocellular carcinoma (HepG2) cells line	Zinc phthalocyanine (ZnPc) with upconversion nanoparticles (UCNs) – (ZnPc-UCNs) 22, 110, 220, 330, 440, 550 mg/mL	Laser VD-IIIA DPSS NIR 980 nm 7 or 14 kJ/cm^2 0.47 W 5 min	HepG2 cells were seeded in tissue culture plate at 10,000 cells/well. After confluency, the cell monolayer was infected with DENV2 with MOI of 10, and incubated for 2 days. Then, concentrations of ZnPc-UCNs were added, incubated in the dark and irradiated.	After 2 days of photoinactivation, the virus titers were analyzed *via* viral plaque assay to DENV-2. For Ad5V post-72 h photoinactivation, an immunofluorescence-based counting method was used to virus titer.	At 440 mg/ml and 550 mg/ml ZnPc-UCN concentrations, virus titer reduced to 2.23 $\log_{10}$ PFU/mL and 2.08 $\log_{10}$ PFU/mL respectively, exhibiting more than 50% reduction in infectious DENV2 titer on cells. The 440 mg/mL ZnPc-UCN concentration showed that only 18.66% HeLa cells was infected with Ad5V, pointing that ZnPc-UCN-PDT is effective to inactivate Ad5V.	ZnPc-UCNs-PDT pointed the nanoparticles increased target specificity and it is promising to the treatment modality for localized viral infections.
		Adenovirus type 5 (Ad5V)	DNA (non-enveloped)	C6/36 cells and HeLa cells	2 h	–	Monolayer of HeLa cells grown on coverslip was inoculated with Ad5V photoinactivated and incubated for 1 h. Then, the excess inocula were removed, cells were washed and reincubated.			
Lhotáková, Y., et al 2012 [50]	Czech Republic	Mouse polyomavirus (strain A2)	DNA (non-enveloped)	Swiss Albino mouse (3T6) fibroblasts	Tetraphenylporphyrin (TPP) 0, 0.001, 0.005 and 0.010 %	Xe lamp UV/VIS 400 nm – 300 W 10, 20 or 30 min	The TPP-PDT effect on mouse polyomavirus and baculovirus were performed with nanofibers materials containing TPP (polyurethane Tecophilic® and polycaprolactone (PCL)) and in water-soluble TPP (TPPS). For this, mouse polyomavirus at 1×10^5 and the recombinant baculovirus at 5×10^4 PFU were	A specific rat monoclonal antibody directed against the large T antigen (for mouse polyomavirus) or a mouse monoclonal antibody against the polyomavirus VP1 protein produced by recombinant baculovirus were added. Unbound antibody was removed by washing and infected cells were visualized by fluorescence microscopy. The values were counted from 5 representative fields containing approximately 130 cells.	The infectivity inhibition with 1 % TPP-doped Tecophilic® and PCL nanofiber textiles after 10 and 30 min of irradiation is similar for both viruses, with reduction around 40 % for mouse polyomavirus and 10 % for baculovirus after 30 min of irradiation. Concentration of TPPS above 0.0.5 % entirely inhibited	The photophysical, photochemical and photovirucidal properties of polymer nanofibers with TPP-PDT and solutions TPPS reveal photovirucidal efficient sources on non-enveloped polyomaviruses and enveloped baculoviruses.
		Baculoviruses	DNA (enveloped)	Spodoptera frugiperda (Sf9) cells	30 min	–				

(*continued on next page*)

Table 1 (*continued*)

Author / Year	Country	Virus	Virus genome type (Virus group)	Cell/sample type	Photosensitizer (PS) Concentration used and time of exposure to PS	Light source / Wavelenght / Fluence / Pontence-density / Time of exposure / Iluminance	Protocol	Measurement of results	Main outcomes	Conclusion
							incubated on nanofibers textiles with TPP and TPPS in the dark, and irradiated. Then, photoinactivated polyomavirus suspensions were added on monolayer of 3T6 cells for 1 h, removed supernatant, DMEM was added, re-incubated for 20 h and fixed. The photoinactivated suspensions of the baculovirus were added on Sf9 cells for 1 h, removed supernatant, the TMN–FH was added and re-incubated for 36 h and fixed.		both viruses. The infectivity of the mouse polyomavirus at 0.001 % TPPS photoinactivated was lower when compared with baculovirus that was more resistant with a decrease to approximately 65 % of infectivity.	
Mohr, H., et al. 2004 [51]	German	West Nile virus (WNV)	RNA (enveloped)	Fresh frozen plasma (FFP)	Methylene blue (MB)	White light	MB was dissolved in 265 ml of FFP and virus suspensions of WNV, HIV-1 and SHV-1 (6.59, 5.83 and 6.56 log $TCID_{50}$) were mixed with the plasma in the dark, and illuminated with white light (for WNV) or yellow light (for WNV, HIV and SHV-1) on different times.	After photoinactivation, the reduction of WNV, HIV-1, and SHV-1 in plasma units were determined by log $TCID_{50}$, and quantitative PCR was used to analyze if the viral RNA was destroyed on plasma infected with WNV.	Complete inactivation >5.5 log_{10} of WNV was achieved by MB (0.8 and 1 μmol/L) with white light (30,000 to 45,000 lux). For themonochromatic yellow light-MB at 0.8 μmol/L MB with a dose at 100 to 200 J/cm^2, it was enough to inactivate the viruses: 5.75 (WNV), 4.99 (HIV-1), and 5.71 log $TCID_{50}$ (SHV-1). The influence of MB–yellow light protoinactivation genome of WNV investigated by real-time PCR, indicated a reduction at 100 J/cm^2 by 93 to 95 %	The WNV is a transfusion-relevant virus that is susceptible to photodynamic treatment in the presence of MB.
		Human immunodeficiency virus (HIV-1)	RNA (enveloped)		0.2, 0.5, 0.8 and 1.0 μmol/L	–				
		Suid herpesvirus 1 (SHV-1, pseudorabiesvirus)	DNA virus (enveloped)		–	0.4 J/cm^2/min – 2, 5 or 10 min 45.000 lux Monochromatic yellow light 590 nm 0 to 200 J/cm^2 – 75 s/10 J/cm^2 – –				

(*continued on next page*)

Table 1 (*continued*)

Author / Year	Country	Virus	Virus genome type (Virus group)	Cell/sample type	Photosensitizer (PS) Concentration used and time of exposure to PS	Light source / Wavelenght / Fluence / Pontence-density / Time of exposure / Iluminance	Protocol	Measurement of results	Main outcomes	Conclusion
Monjo, A. L.-A., et al. 2018 [34]	Canada	Herpes simplex viruses (HSV-1) and (HSV-2) Vesicular stomatitis virus (VSV) GFP-Adenovirus 5 vector (AdV5-GFP)	DNA (enveloped) RNA (enveloped) DNA (non-enveloped)	Immortal human of Herietta Lacks (HeLa) cells Human embryonic kidney (HEK293A) cells African green monkey kidney (Vero) cells	Ortoquin 0.01, 0.05, 0.1, 0.5 and 1.0 μg/mL –	LED White light – 12.6 J/cm^2 21 mW/cm^2 5 or 10 min –	HSV-1, HSV-2, VSV and AdV5-GFP were submitted at concentrations Ortoquin-PDT. Two conditions were used to irradiate:, a clear microcentrifuge tube labeled as "light" (VWR) or a black termed as "dark". After photoinactivation, suspensions of HSV-1 and HSV-2 were added on HeLa cells (4.5×10^5 cells/mL), VSV were added on Vero cells ($2.5' \times 10^5$ cells/mL), and AdV5-GFP were added on HEK293A cells (4.5×10^5 cells/mL), for 1 h with shaking every 10 min.	After one day, cells infected with virus were fixed with crystal violet. Inactivation of virus was determined by PFU.	and at 300 J/cm^2 by 95 to 98 %. Orthoquin-PDT (0.5 and 1.0 μg/mL), showed a complete reduction of PFU for HSV-1, HSV-2, and VSV. For AdV5-GFP a count reduction from 100 to 20 PFU (0.5 μg/mL) and from 100 to 5 PFU (1.0 μg/mL) were obtained in a light-dependent manner (light). The effect to light-independent (dark) manner of Orthoquin reduced almost completely at concetration 0.5 and 1.0 μg/mL for HSV-1, HSV-2 and VSV. For AdV5-GFP, a count reduction from 100 to 60 PFU was demonstraded at 1.0 μg/mL.	The results pointed that Orthoquin posesses light-dependent, as well as light-independent behavior at higher concentrations when evaluted on viruses tested. However, Orthoquin may be an alternative for inactivation of HSV in surface lesions, which could be be effective against drug-resistant strains and mitigate the emergence of resistance.
Namvar, M. A., et al. 2019 [52]	Iran	Herpes Simplex Viruses 1 (HSV-1)	DNA (enveloped)	African green monkey kidney (Vero) cells	Indocyanine green (ICG) 0.1 mg/mL 5 min –	Infra-red diode lasers 810 and 940 nm 78 J/cm^2 500 mW/cm^2 60 s –	Suspension of clinical sample HSV-1 was added on Vero cells (3×10^5/mL) to absorb the viruses for 1 hour. Then, ICG was added, incubated and irradiated to diode laser at 810 or 940 nm.	To determine virus inactivation qRT-PCR was performed.	ICG irradiated with 810 and 940 nm diode laser significantly reduced the count of HSV1/mL 1.548×10^5 to irradiation at 810 nm and to irradiation at 940 nm 2.484×10^5 in relation to control (9.0×10^5).	The ICG-PDT may be an effective treatment for clinical herpetic lesions.
Randazzo, W., et al. 2016 [53]	Spain	Feline calicivirus (FCV) Murine norovirus (MNV)	RNA (non-enveloped) RNA (non-enveloped)	Cat kidney (CRFK) cells Murine macrophage (RAW 264.7) cell	Curcumin (CUR) 5, 50, 100 μg/mL –	LED blue light 464 to 476 nm 3 J/cm^2 – 30 or 120 min –	Virus suspensions (6–7 log $TCID_{50}$/mL) added with different concentrations of CUR) were illuminated with LED. After	Infectious viruses photoinactivated were determined by $TCID_{50}$.	MNV showed inactivation rates below 1 log $TCID_{50}$/mL, slight reductions on MNV infectivity. For FCV photoactivated with	The CUR-PDT may be an alternative natural additive to reduce viral contamination.

(*continued on next page*)

Table 1 (*continued*)

Author / Year	Country	Virus	Virus genome type (Virus group)	Cell/sample type	Photosensitizer (PS) Concentration used and time of exposure to PS	Light source / Wavelenght / Fluence / Pontence-density / Time of exposure / Iluminance	Protocol	Measurement of results	Main outcomes	Conclusion
							photoinactivation, virus suspensions MNV-1 were inoculated into monolayes of RAW 264.7 cell, and FCV suspensions into monolayes of CRFK cells.		50 μg/mL CUR at 37 °C resulted in a complete inactivation of the virus, or at least, below the detection limit of the assay, 1.15 log, reduced almost 5 log $TCID_{50}$/mL.	
Sawyer, L., et al. 2007 [54]	United Stated	Human Parvovirus B19 (B19)	DNA (non-enveloped)	Human platelet concentrates (PLT)	Amotosalen-HCl 150 μmol/L 5 to 90 min	UVA light (UVA) – 3.0 J/cm^2 – – –	The Amotosalen-HCl was added in PLT B19-infected plasmas with 1×10^{1111} to 1×10^{10} geq/mL), incubated at different times and temperatures, and irradiated.	B19 inactivation was calculated as log reduction with the formula Log reduction = log (pretreatment B19 titer/ posttreatment B19 titer).	The preincubation of 60, 75 and 90 min before photoinactivation resulted in 5.3 log, 5.6 log and 5.8 log titer/SFUs/mL of B19 reduction.	The photoinactivation with Amotosalen pointed the ability to inactivate virus B19 in a blood product.
Singh, Y., et al 2006 [55]	United Stated	Human immunodeficiency virus-type 1 (HIV-1) Human T-cell lymphotropic virus-I and II (HTLV-I and HTLV-II) Hepatitis B virus (HBV) Hepatitis C virus (HCV) West Nile virus (WNV) Severe acute respiratory syndrome coronavirus (SARS-CoV) Duck hepatitis B virus (DHBV)	RNA (enveloped) RNA (enveloped) DNA (enveloped) RNA (enveloped) RNA (enveloped) RNA (enveloped) DNA (enveloped)	Fresh frozen plasma (FFP)	Amotosalen 150 μmol/L – –	UVA light (UVA) – 3.0 J/cm^2 – 7 to 9 min –	The volume of FFP was composed of 585 ml of plasma and 15 ml of amotosalen solution, added the suspensions virus of 10^4 to 10^6, that were agitated during irradiation. Being infected with: HIV-1, cell-free $10^{6.1}$ PFU/mL, HIV-1, cell-associated $10^{5.9}$PFU/mL, HTLV-I 10^4FFU/mL, HTLV-II $10^{4.7}$FFU/mL, HBV $10^{4.5}$ CID_{50}/unit, HCV $10^{4.5}$ CID_{50}/unit, DHBV $10^{5.6}ID_{50}$/mL,	Photoinactivation of virus was calculated as log-reduction with the formula Log-reduction = log (pre-PCT titer/post-PCT titer)	The PCT showed a reduction of HIV-1, cell-free $>6.8 \pm 0.1$ PFU/mL, HIV-1, cell-associated $>6.4 \pm 0.2$ PFU/mL, HTLV-I $\geq 4.5 \pm 0.7$ FFU/mL, HTLV-II $>5.7 \pm 0.1$ FFU/mL, HBV > 4.5 CID_{50}/unit, HCV > 4.5 CID_{50}/unit, DHBV 4.4-4.5 ID_{50}/mL, BVDV $\geq 6.0 \pm 0.03$ PFU/mL, WNV $\geq 6.8 \pm 0.5$ PFU/mL, SARS-CoV $\geq 5.5 \pm 0.1$ PFU/mL, HAdV-5 $\geq 6.8 \pm 0.4$ PFU/mL, BTV 5.1 ± 0.2 PFU/mL.	PCT with amotosalen and UVA light is effective against a range of virus enveloped or non-enveloped in plasma.

(*continued on next page*)

Table 1 (*continued*)

Author / Year	Country	Virus	Virus genome type (Virus group)	Cell/sample type	Photosensitizer (PS) Concentration used and time of exposure to PS	Light source / Wavelenght / Fluence / Pontence-density / Time of exposure / Iluminance	Protocol	Measurement of results	Main outcomes	Conclusion
		Bovine viral diarrhea virus (BVDV) Bluetongue vírus (BTV) Human adenovirus 5 (HAdV-5)	RNA (enveloped) RNA (non-enveloped) DNA (non-enveloped)				BVDV $10^{4.5}$ PFU/mL, WNV $10^{6.3}$ PFU/mL, SARS-CoV 10^{4} PFU/mL, HAdV-5 $10^{5.5}$ PFU/mL, BTV 10^{4} PFU/mL			
Tomé, J. P. C., et al. 2007 [56]	Portugal	Herpes simplex virus type 1 (HSV-1)	DNA (enveloped)	African green monkey kidney (Vero) cells	Profirins derivate: Neutral 1b and Cationic tripyridylporphyrin-D-galactose 3b 0.02 μM 30 min	White light <540nm – 15 min 50 mW/cm^2 –	Confluent Vero cells at 10^5 cells/well were infected with a suspension of HSV-1 at 10^7 PFU/mL. Different post-adsorption times of virus on cells at 0, 2, 4, and 16 h were analyzed, and also the influence of the PS, incubated in the dark and irradiation to addition time on virus yield during infection.	The virus yield was determined by titration of samples collected 24 hours post-infection. The inhibition of HSV-1 yield was calcuted by % and ± SD compared with control.	The neutral compound 1b is more efficient at later times of the viral replication cycle assayed at 4 and 16 h post-infection, showing an inhibition of 93.6 and 95.7 %. The cationic compound 3b highly inhibits the viral yield at all the addition times evaluated, and similarly to compound 1b, the highest inhibition is also observed at the addition time 16 h post-adsorption with inhibition of 99.8 %.	Effects of compounds 1b and 3b on virus yield photoinactivated in differents time pointed a significant inhibition on HSV-1 at non-cytotoxic concentrations, evidencing the potential anti-herpetic activity.
Trannoy, L. L., et al. 2006 [57]	Netherlands	Pseudorabies virus (PRV) Canine parvovirus (CPV) Bovine viral diarrhea virus (BVDV) Cell-associated human immunodeficiency virus (CA-HIV) Extracellular human	DNA (enveloped) DNA (non-enveloped) RNA (enveloped) RNA (enveloped) RNA (enveloped)	Red cell concentrates (RCC)	Cationic porphyrin, mono-phenyl-tri-(N-methyl-4-pyridyl)-porphyrin chloride [Tri-P(4)] 25 μM 5 min	Halogen lamp red light >600 nm 360 kJ/m^2 100 W/m^2 15, 30 or 60 min –	Virus titers were calculated as $TCID_{50}$/mL, of which 10^8 to PRV, 10^6 to BVDV and E-HIV, 10^8 to CA-HIV and 10^7 $TCID_{50}$ to CPV. Tri-P(4) was added to viruses in the RCC, incubated in the dark and illuminated.	Reduction factors (RF) were calculated by the formula: RF = $\log_{10}$ (total amount of virus spiked as derived from the reference sample ÷ total amount of virus recovered from the treated sample).	Tri-P(4) and irradiation pointed a reduction of ≥ 4.6 $\log_{10}$ to PRV and > 5.5 $\log_{10}$ inactivation of BVDV and E-HIV, with 60 min irradiated. The inactivation of CA-HIV was limited to ≈ 2 $\log_{10}$, while the CPV was completely resistant to the treatment.	Tri-P(4) and PDT on RCC inactivates a wide range of pathogens, that may be considered as a feasible approach to sterilize red cell products.

(*continued on next page*)

Table 1 (*continued*)

Author / Year	Country	Virus	Virus genome type (Virus group)	Cell/sample type	Photosensitizer (PS) Concentration used and time of exposure to PS	Light source / Wavelenght / Fluence / Pontence-density / Time of exposure / Iluminance	Protocol	Measurement of results	Main outcomes	Conclusion
		immunodeficiency virus (E-HIV)								
Vargas, F., et al. 2008 [58]	Venezuela	Human immunodeficiency virus (HIV-1)	RNA (enveloped)	MT4 cells	Meso-tetraphenylsulfonated porphyrins (TPPMS4) complexes: TPPFeS4 TPPMnS4 TPPPdS4 TPPZnS4 mol –	UVA-Vis 320−600 nm 4.5 J/cm^2 3.3 mW/cm^2 30 min 45.575 lux/sec	The MT4 cells (120000 cells/well) were seeded in plates, added the IC50 of compounds, then were infected with HIV-1 and illuminated. After 12 h, the supernatant were changed and the cells washed, and reseeded.	The virus production was analyzed at 72, 96 and 120 h by collection of supernatant and determined by enzyme-linked immunosorbent assay in ELISA using level of p24 antigen.	The photoinactivation showed antiviral activity of the complexes TPPFeS4 (inhibition 80–85 % after 120 h post-irradiation), TPPMnS4 (inhibition of almost 98%), TPPPdS4 (over 70% inhibition) and TPPZnS4 (inhibition of almost 98%) on the inhibition of HIV-1, and the cellular viability remained during the irradiation process.	The inhibition has been determined in the viral growth (HIV-1) when irradiated with complexes: TPPFeS4, TPPMnS4, TPPPdS4 and TPPZnS4, and the cellular viability was unaltered.
Va, F., et al. 2013 [35]	United States of America	Human immunodeficiency virus-1 (HIV-1)	RNA (enveloped)	TZM-bl cells	LJ001 (rhodanine derivative)	White fluorescente light	MOIs within the linear range or at dilutions compatible with plaque assay (0.2-0.4) were incubated with serial dilution of the compounds LJ001, JL103, L118 and JL122 exposed at white fluorescent light.	IC_{50} was calculated by non-linear regression analysis with variable slopes with constraints set for the max. and min. at respectively 100 and 0%. For JL118 and JL122, IC_{50} measured after 10 min of light exposure.	Effect of LJ001-PDT on HIV, HSV, NDV, H1N1, SFV, VSV, RABV, NiV, CMV, RVFV, EBOV, HeV, showed a IC_{50} of 133, 20, 95, 25.7, 537, 298, 5288, 475, 147, 20, 900, 18 nM, and for JL103-PDT 13, 2, 4, 1.7, 44, 11, 260, 3.9, 5, 3, 185, nM, respectively to each virus. The viruses HIV, HSV and NDV were also photoinactivated with JL118-PDT and JL122-PDT, exhibiting IC_{50} in concentrations 11.7, 10.1, 2.1 nM to JL118, and 64, 2.4, 0,9 nM to JL122. For AdV5 the photoinactivation with PS did not show effect.	The optimization of LJ001 led to a new class of membrane-targeted photosensitizers (oxazolidine-2,4-dithiones) with increased antiviral efficacy.
	Portugal	Newcastle disease vírus (NDV)	RNA (enveloped)	African green monkey kidney (Vero) cell line	JL103 (oxazolidine-2,4-dithione)	–				
	Singapore	Hendra virus (HeV)	RNA (enveloped)	African green monkey kidney (Vero) cell line	JL118 oxazolidine-2,4-dithione)	–				
	United Kingdom	Nipah virus Malaysia (NiV)	RNA (enveloped)	Baby hamster kidney cell (BHK-21)	JL122 (oxazolidine-2,4-dithione)*	85 W				
	Switzerland	Influenza A A/PR/8/34 (H1N1)	RNA (enveloped)		–	–				
		Ebola Zaire (EBOV)	RNA (enveloped)							
		Rift Valley fever MP-12 (RVFV)	RNA (enveloped)							
		Semliki forest virus (SFV)	RNA (enveloped)							
		Vesicular stomatitis virus (VSV)	RNA (enveloped)							
		Cytomegalovirus (CMV)	DNA (enveloped)							
		Herpes simplex virus-1 (HSV-1)	DNA (enveloped)							

(*continued on next page*)

Table 1 (*continued*)

Author / Year	Country	Virus	Virus genome type (Virus group)	Cell/sample type	Photosensitizer (PS) Concentration used and time of exposure to PS	Light source / Wavelenght / Fluence / Pontence-density / Time of exposure / Iluminance	Protocol	Measurement of results	Main outcomes	Conclusion
Wu, J., et al. 2015 [59]	China	Rabies virus (RABV) Adenovirus serotype 5 (Ad5) Murine norovirus 1 (MNV-1)	RNA (enveloped) DNA (non-enveloped) RNA (non-enveloped)	RAW 264.7 mouse monocytes and macrophages	Curcumin (CUR) 5 μM, 10 μM and 20 μM –	Blue LED light 470 nm 3.6 J/cm^2 0.06 W/cm^2 60 s –	The MNV-1 was incubated with concentrations of CUR and irradiated. The suspension photoinactivated was incubated with monolayers of RAW 264.7 mouse monocytes/ macrophages.	After 48 h of incubation, viral titer was determined by PFU/mL.	Reductions of 1.32 log, and > 3 log PFU/mL wit concentrations of 5 μM, and 20 μM of CUR-PDT, respectively.	CUR-PDT was efficient to photoinactivate MVN-1.
Xu, L., et al. 2019 [60]	China	Human T lymphotropic virus (HTLV -1)	RNA (envoloped)	HPB-ATL-T MT-2 C8166 TL-Om1	Hypericin (Hy) 2.5, 5, 6.25, 10, 12.5, 20, 25, 40, 50, 80, 100 and 200 ng/mL 16 h	Visible light 520–750 nm 11.28 J/cm^2 – 30 min –	HTLV-1-infected T-cell lines were incubated in the dark with concentrations of Hy, subsequently, were illuminated and re-incubated in the dark.	After 24 h of photoinactivation, cell growth was evaluated by MTT assay, and determined by IC_{50}.	The Hy-PDT resulted in a dose-dependent growth inhibition to all cell lines tested. the IC_{50} to HPB-ATL-T, MT-2, C8166 and TL-Om1 were 52.98 ± 10.11, 52.86 ± 10.57, 43.02 ± 9.25, 37.88 ± 9.36, and 19.04 ± 6.22 ng/mL, respectively.	Hy-PDT is highly efective against ATL cells by induction of suppression of viral transcription, being a promising therapy for ATL.
Yin, H., et al. 2012 [61]	China	Human immunodeficiency virus (HIV)	RNA (enveloped)	C8166 cells	Hematoporphyrin monomethyl ether (HMME) 5, 10, 20, 30, 40, 50, 60, 70, 80, 90 and 100 μg/mL 40 min	Laser 630 nm 1.2 J/cm^2 20 mW/cm^2 1 min –	HIV-1 strains were incubated with HMME concentrations and irradiated. Then,the suspensions photoinactivated were used to infect C8166 cells (10^5/ mL, MOI 0.3) and incubated for 3 days.	After 3 days, the viral inibhition was determined by level of p24 antigen in the culture supernatant tested by enzyme-linked immunosorbent assay (ELISA).	HMME (100 μg/mL) and PDT pointed virus inactivation rates at almost 100 %.	HMME-PDT pointed that most of HIV strains are responsive, which represents a promising treatment for AIDS patients.
Zverev, V. V., et al. 2016 [62]	Russia	Herpes simplex virus (HSV)	DNA (enveloped)	African Green Monkey kidney (Vero) cell line	Fotoditazine 0, 10, 50, 100, and 200 μg/Ml 30 min or 1.5 h	Laser light 662 nm 0.285, 0.57, 1.8, 3.42, and 10.62 J/cm^2 0.06 Wt/cm^2 5, 10, or 30 sec and 1 or 3 min	Concentrations of Fotoditazine were added on HSV-1, and incubated for 30 min or 1.5 h and irradiated, or the suspensions were immediately irradiated. After	After 24 h, the inhibition of virus activity after photoinactivation was determined based on the inhibition of viral cytopathic activity in cultured cells, measured as the cytopathic dose (lg TCD_{50}/mL).	Photosensitizer doses of 50 μg/mL or more with decreased HSV-1 viral titer by 1000-fold or greater (1.5–2.5 orders of magnitude).	Fotoditazine-PDT was effective for the treatment of HSV-infected culture cells.

(*continued on next page*)

Table 1 (*continued*)

Author / Year	Country	Virus	Virus genome type (Virus group)	Cell/sample type	Photosensitizer (PS) Concentration used and time of exposure to PS	Light source / Wavelenght / Fluence / Pontence-density / Time of exposure / Iluminance	Protocol	Measurement of results	Main outcomes	Conclusion
						–	photoinactivation, the suspensions were added to Vero cells culture immediately or 1 h or 3 h post-PDT, for 24 h.			

Geq: genome titers of virus, FFU/mL : foci-forming units per milliliter, ID_{50} : infectious dose necessary for infection of 50 % of inoculated, CID_{50}: infectious dose necessary for infection of 50 % of inoculated, LED: Light-emitting diodes, KLV: killing log value ($lgN_0 = lgN_\times / N_0$ is the initial virus titration and $N_\times$ is the average titration), MOI: Multiplicity of infection, PCT: Photochemical treatment, PFU: plaque-forming unit, SFU(s) : spotforming unit(s), IC_{50}: half maximum inhibitory concentration, $TCID_{50}$: tissue culture infective dose. Measured with 50 % tissue culture infectious dose ($TCID_{50}$) –* Kaerber and Spearma ($RF = \log_{10}$(total amount of virus spiked as derived from the reference sample ÷ total amount of virus recovered from thetreated sample)), TEM: Transmission electron microscopy, qRT-PCR: Real-time polymerase chain reaction, MTT: 3-(4, 5-dimethylthiazol-2-yl)-2, 5-diphenyl tetrazolium bromide.

* Not describe in article.

Table 2
In vivo studies of PDT on viruses from 2004 to 2020.

Author / Year	Country	Virus	Virus genome type (Virus group)	Animal used	Photosensitizer (PS) / Concentration used / route of administration and time of exposure to PS	Light source / Wavelenght / Fluence / Pontence-density/ Time of exposure	Treatment protocol	Measurement of results	Treatment outcome	Conclusion
Lee, R. G., et al. 2010 [48]	United States of America	Cottontail rabbit papillomavirus (CRPV)	DNA (non-enveloped)	New Zealand White rabbits and CB17-SCID mice	Phthalocyanine (Pc 4) 0.6 or 1.0 mg/kg Intravenously *via* tail-vein 48 h	Diode laser 675 nm 100 or 150 J/cm^2 75 mW/cm^2 –	Full-thickness skin grafts were harvested from the back of the ears of the rabbits, and placed onto 7-mm wounds on the backs of CB-17 SCID mice (n = 26). After 3 weeks, the epithelium was inoculated with undiluted thawed 4 μl CRPV suspension, scarified through a 27-gauge hypodermic needle and added more 4 μl of the CRPV. Cutaneous papilloma were grown by approximately 4 weeks (score 5). Then, Pc 4-PDT was administered at sessions with an interval of 48 h.	The regression curve of papilloma growth curve was evaluated after 7 days with a microcaliper to measure and compare the mean slope of treated and control groups. The volume was calculated using the formula 4/3π × ½ length × ½ width × ½ height and recorded.	Tumor growth was reduced in the group treated with 1.0 mg/kg Pc 4 and 150 J/cm^2 laser light, animals treated 13/15 (87%) has completely regressed.	The Pc 4-PDT may be a potential treatment for HPV-induced papilloma.
Lim, M. E., et al. 2012 [49]	Singapore	Dengue virus serotype 2 (DENV2)	RNA (enveloped)	BALB/c mice	Zinc phthalocyanine with upconversion nanoparticles (ZnPc-UCNs) 4, 44 or 440 mg/mL Intracranially –	VD-IIIA DPSS NIR laser 980 nm 14 kJ/cm^2 0.47 W 10 min	Seven groups of BALB/c mice (n = 6) 1 to 2-day-old were used. Three groups of the suckling mice were inoculated intracranially with DENV2 (6.37 $\log_{10}$ PFU/mL) and treated with concentrations ZnPc-UCNs-PDT. The mice were observed for signs of dengue viremia for 15 days.	Mortality of the suckling mice was recorded and a Kaplane–Meier survival curve plotted.	The highest ZnPc-UCN concentration used (440 mg/mL) showed the survivability of the suckling mice was 100 % until the last day of observation, similar to negative control.	The use of ZnPc-UCNs-PDT in treatment modality for localized viral infections is promising.
Wu, J., et al. 2015 [59]	China	Murine norovirus 1 (MNV-1)	RNA (non-enveloped)	Oyster	Curcumin (CUR) 5 μM, 10 μM, 20 μM – –	LED Blue light 470 nm 3.6 J/cm^2 0.06 W/cm^2 60 s	Groups oyster (n = 6) were treated with concentrations of Cur and irradiated into an artificial seawater system (salinity	The oysters' intestine were removed and dissected out.	The oyster group treated with 10 μM of Cur-PDT has a reduction 0.76 $\log_{10}$ PFU/mL, and for 20 μM, reduction of	The treatment of oysters Cur-PDT is a potentially efficacious and cost-effective

(*continued on next page*)

Table 2 (*continued*)

Author / Year	Country	Virus	Virus genome type (Virus group)	Animal used	Photosensitizer (PS) / Concentration used / route of administration and time of exposure to PS	Light source / Wavelenght / Fluence / Pontence-density/ Time of exposure	Treatment protocol	Measurement of results	Treatment outcome	Conclusion
							3.3 %) for 6 h at 10 °C.		1.15 $\log_{10}$ PFU/mL.	method to inactivate food-borne NoV.

PFU: plaque-forming unit.

articles (Table 1), and one article used two different sources [49]. White light was the most frequently light source used in the articles included, representing 19.2 % (n = 5/26) [32,33,48,49,54]. Subsequently, UVA light presented a rate of 15.3 % [37,52,53,56] (n = 4/26). The Laser light [47,59,60] and Halogen lamp [39,42,44] presented a rate of 11.5 % (n = 3/26). Tungsten lamp [36,43], Blue LED light [51,57] and LED [41,45], were equivalent to 7.6 % (n = 2/26). Finally, Double-sided panels of Edison diodes [38], Monochromatic yellow light [49], Infra-red diode lasers [50], Fluorescent lamp [40], Red light [55] and Visible light [58] were presented 3.8 % (n = 1/26).

In vivo studies analyzed included 3 different light sources as shown in Table 2, corresponding to 33.3 % (n = 1/3) to Blue LED light source [57], 33.3 % (n = 2/3) to VD-IIIA DPSS NIR laser [47] and 33.3 % (n = 3/3) Diode Laser [46] respectively.

3.2.3. Analysis of main outcomes

Regarding models for presenting the results of selected *in vitro* articles (n = 26), 12 alternative techniques to quantify the effect of photoinactivation on viruses were found. The most frequently used techniques was plaque-forming units (PFU) corresponding at 19.2 % (n = 5/26) [32,40,47,53,57], and 19.2 % (n = 5/26) for analysis of tissue culture infective dose (TCID50) [44,49,51,55,60], to both the logarithmic reduction was used. Successively, the half maximum inhibitory concentration (IC50), presented a rate of 15.3 % (n = 4/26) [33,42,56,58]. Evaluation by titer virus reduction was equivalent to 11.4 % (n = 3/26) when represented by logarithmic reduction [38,39,41], in other articles the titer virus reduction was quantified in percent, corresponding to 7.6 % (n = 2/26) [54,59]. At last, the subsequent techniques were found only once in articles, corresponding to 3.9 % (n = 1/26) for crystal violet evaluate [36], 3.9 % (n = 1/26) by flow cytometry (in percent) [43], 3.9 % (n = 1/26) at spot forming unit (SFU) represented by logarithmic reduction [52], 3.9 % (n = 1/26) quantification of the viral genome by real-time polymerase chain reaction (qRT-PCR) [50], 3.9 % (n = 1/26) to immunocytofluorescence counts [45], 3.9 % (n = 1/26) fluorescence microscopy counts [48], and 3.9 % (n = 1/26) quantify by luminescence unit counts [37] respectively (Table 1).

For *in vivo* studies the distinct evaluation parameters were observed (Table 2), as follows, regression curve of papilloma growth curve (33.3 %; n = 1/3) [46], reduction logarithmic by PFU (33.3 %; n = 1/3) [57], and the Kaplane-Meier survival curve (33.3 %; n = 1/3) [47].

3.3. Effect of photodynamic therapy on Viruses

3.3.1. RNA viruses (enveloped and non-enveloped)

Overall, 17 studies investigated PDT on RNA viruses, as shown in Table 1. From that, 15 were in enveloped viruses, belonging to nine families: *Flaviviridae* (Bovine viral diarrhea virus -BVDV, Dengue virus - DENV, Hepatitis C virus - HCV and West Nile virus - WNV), *Filoviridae* (Zaire Ebola virus - EBOV), *Phenuiviridae* (Rift Valley Fever - RVF), *Coronaviridae* (Coronavirus - SARS-CoV), *Retroviridae* (Human Immunodeficiency virus - HIV, Human T lymphotropic virus - HTLV), *Orthomyxoviridae* (Influenza A virus - H1N1 and Avian influenza A virus - H5N8), *Paramyxoviridae* (Hendra virus - HeV, Newcastle disease virus - NDV, Malaysia Nipah virus - NiV), *Rhabdoviridae* (Vesicular Stomatitis Indiana virus - VSV and Rabies virus - RABV) and *Togaviridae* (Semliki Forest virus - SFV) [61]).

The authors Cruz-Oliveira et al. [40] and Yin et al. [59] used derivatives from porphyrin (as PS) to demonstrate the antiviral activity of PDT. Cruz-Oliveira et al. [40] investigated protoporphyrin IX, Zn-protoporphyrin IX, and mesoporphyrin IX, against VSV, as possible broad-spectrum antiviral drugs. The three PS showed a dose-dependent viral inactivation, but the activity was potentialized 5 to 500-times when irradiated with a fluorescent lamp (30 W), promoting total VSV inactivation [40]. In another study, the authors investigated the PDT mediated by hematoporphyrin monomethyl ether (HMME) against cell-free HIV. HMME-PDT was efficient to inactivate all strains tested: HIV-1, HIV-2, resistant HIV, and HIV clinical. Efficacy of PDT against HIV was proportional to HMME concentration and energy density. However, it was inversely proportional to the power density. Increased power density (80 mW/cm^2) resulted in the increased virus death probably due to the thermal injury from the laser [59].

Photosensitizers derivatives from porphyrin mediated PDT were tested for application in blood sterilization [55,56]. Among the synthetic mesotetraphenylsulfonated porphyrins (TPPMS4) complexes tested against HIV-1. The TPPFeS4, TPPMnS4, TPPPdS4, TPPZnS4 compounds showed high viral inactivation capacity (> 70 %) which was related to higher production of ROS [56]. Trannoy et al. [55] evaluated PDT mediated by the cationic porphyrin, [Tri-P(4)] to inactivating RNA enveloped viruses (BVDV, Cell-associated human immunodeficiency virus - CA-HIV and Extracellular human immunodeficiency virus - E-HIV) in red cell concentrates (RCC). They also evaluated the associated effect on *in vitro* red blood cells quality. Sixty minutes of halogen lamp red light irradiation in combination of 25 μM Tri-P(4) resulted in > 5·5 $\log_{10}$ inactivation of BVDV and E-HIV, while CA-HIV showed less sensitivity (inactivation of ≈ 2 $\log_{10}$), this because Tri-P(4) does not enter the cell. However, the authors stated, some problems such as improving the protection of the red cells, as well as the media for preserving RBC integrity that has to be solved before considering this approach is proper to sterilize red cell products.

Studies that analyzed activities of conjugates of phthalocyanines as PS [42,44,47] demonstrated effective inactivation of RNA enveloped viruses. The effect of a series of zinc(II) phthalocyanines conjugated with an oligolysine chain in the PDT with a dose of 48 J/cm^2 of halogen lamp against different viruses was displayed. The study used H1N1 (enveloped viruses) and Cox B1 (a model of non-enveloped viruses). H1N1 was efficiently inactivated by all three PS with low concentrations (0.05 to 0.17 nM). However, the IC_{50} for Cox B1 could not be determined up to 8 μM. This difference in phototoxicity efficacy has been attributed due to outer lipid membrane and capsid proteins in enveloped viruses that are the main targets for photodamage [42]. Other research performed an ultrastructural study of morphological differences between intact and photodynamically inactivated virions after PDT with Octacationic

octakis (cholinyl) zinc phthalocyanine followed by 12 J/cm^2 of light dose of halogen lamp irradiation using the RNA enveloped H5N8. The PDT was able to completely inactivate this virus without destroying it. Through the transmission electron microscopy images, it was possible to observe that PDT decreased glycoproteins from the virions membrane surface (spikes) making them non-infectious [44]. Lim et al. [47] presented the use of near-infrared (NIR) -to-visible upconversion nanoparticles (UNCS) as an alternative to overcome issues in PDT, such as hydrophobicity of photosensitizers and limited tissue penetration ability of the light sources. This approach associated with the use of ZnPc as PS, showed through *in vitro* (Table 1) and *in vivo* (Table 2) experiments, that DENV (RNA enveloped virus) becomes non-infective after ZnPc-UCN-PDT in cells culture and in a murine model.

Belanger et al. [37] used three different naphthalene derivatives (AzNAP, DAN, DINAP) and a diazidobiphenyl compound (DABIPH) followed by UVA irradiation for 2 min (the total dose light used was not informed) which promoted total HIV inactivation evaluated by luciferase assay. These PS are hydrophobic UV-activable compounds that selectively label transmembrane proteins to inactivate enveloped viruses. Controls non-azide did not have effectiveness on viral infectivity, showing that the presence of the azide is necessary for viral inactivation. These results demonstrated that the surface antigenic structures were preserved which is favorable for vaccine preparations.

Vigant et al. [33] showed broad-spectrum antiviral activity *in vitro* of LJ001, a membrane-targeted PS. The authors performed a substitution (oxygen in the ring) in LJ001, that led to an oxazolidine-2,4-dithione named JL103. Thus, JL103 showed an increased ability to generate $^1O_2$ at a higher rate than LJ001 and, consequently, increased anti-viral capacity with lower IC_{50} for all RNA enveloped viruses tested (HIV, NDV, HeV, NiV, H1N1, EBOV, RVFV, SFV, VSV and RABV).

The effect of virus photoinactivation in plasma with Amotosalen and 3 J/cm^2 of UVA light has been evaluated. This study approached sixRNA enveloped viruses (HIV, HTLV, HCV, WNV, SARS-CoV, BVDV) and one RNA non-enveloped virus (BTV) presented significant virus log reductions in all viruses tested. This treatment exhibited efficiency in eliminating pathogens in the plasma with the benefit of the maintenance of functionality. This is the only study so far that approached PDT against SARS-CoV [53].

The MB-PDT was tested in two articles [41,49] that showed efficiency in the photoinactivation of pathogens present in fresh frozen plasma (FFP) and in suspension. Huang et al. [49] analyzed MB-PDT that was affected by four factors: concentration of PS, illumination intensity of light source, illumination distance, and time. The most efficient inhibition of DENV virus was achieved by the combination of MB 1.0 μg/ml, at 2.5 m and 5 min of irradiation, leading to complete inactivation (≈ 6.30 virus titer). As well, the MB white light (for WNV) or low-pressure sodium lamps emitting monochromatic yellow light (for WNV and HIV) for photoinactivate FFP were tested. Using white light, the counting of WNV was below the limit of detection with 1 mmol/L MB and 2 min of irradiation. Otherwise, with the yellow light, WNV and HIV were completely inactivated with 0.8 μmol/L of MB and 20–40 J/cm^2. WNV showed to be very sensitive, being almost completely inactivated with MB even when exposed to ambient light (1 h) [41].

In another study describing a method for inactivation of viruses in the preparations of the plasma from donor blood, the use of SPFPS PS followed by irradiation period totalizing at least 324 J/cm^2 was able to completely inactivate H1N1 virus-containing albumin solution with high initial titer. The advantage of this method was the absence of cytotoxicity and the PS could be easily separated from the product by filtration or centrifugation of the medium [38].

The Orthoquin, a botanical plant extract used as PS with antimicrobial properties was evaluated. The VSV inoculum was incubated with Orthoquin (concentrations ranging from 0.01 to 1 μg/mL) in clear or opaque tubes (black), followed by 65 W LED light irradiation for 5 min. No significant difference was observed between samples from clear or opaque tubes, demonstrating that light exposure did not improve antiviral activity [32].

Xu et al. [58] evaluated Hy mediated by PDT against Adult T-cell leukemia (ATL) cells (aggressive neoplasm caused by HTLV-1) and found that all HTLV-1-positive cell lines (HPB-ATL-T, MT-2, C8166, and TL-Om1) and HTLV-1-negative T-cell line (CEM-T4) displayed growth inhibition after Hy-PDT. However, Hy-PDT had no effect in CD4 + T lymphocytes from healthy donors. Hy-PDT suppressed the proliferation of ATL cells mainly through p53 signaling activation that induced apoptotic processes.

From the 17 studies that investigated PDT on RNA viruses, four were in non-enveloped viruses, belonging to three families: *Reoviridae* (Bluetongue virus - BTV), *Picornaviridae* (Coxsackievirus - Cox B1), and *Caliciviridae* (Feline calicivirus - FCV and Murine norovirus - MNV-1) [61]. From these, two studies also approached RNA enveloped viruses and showed that, comparatively, PDT in these conditions were more effective over enveloped viruses than non-enveloped ones, as mentioned before [42,53]. The other two studies were exclusively in non-enveloped viruses and used CUR as PS and LED blue light [51,57], being that the later was the only among the studies with RNA-non enveloped viruses to apply PDT in an *in vivo* model. Both studies focus on the use of PDT by the seafood industry and used MNV-1 as a surrogate of human norovirus (NoV). It is important to highlight that studies with CUR still need to improve to consider the organoleptic characteristics for use by the industry. Wu et al. used PDT mediated by CUR and LED blue light (3.6 J/cm^2) against MNV-1. This study inactivated MNV-1 in buffers (reduction >3 $\log_{10}$ PFU/mL at a curcumin concentration of 20μM) and also in oysters (reduction of 1.15 $\log_{10}$ PFU/mL at a curcumin concentration of 20μM). The results *in vitro* (Table 1) and *in vivo* (Table 2) demonstrated that virus inactivation was in a dose-dependent manner. In addition, the study showed that CUR-PDT destroyed the integrity of the viral nucleic acid and the stability of viral capsid proteins [57]. In another study, two norovirus surrogates: MNV-1 and FCV were used. The PDT was performed *in vitro* with curcumin and LED blue light. The study showed that FCV was more sensitive to CUR-PDT than MNV-1. Furthermore, when the treatment was assessed at 37 °C, it was possible to observe an increase in the reduction of virus infectivity for FCV at room temperature, 5 μg/ mL of CUR reduced FCV titers by 1.75 $\log_{10}$ TCID50/mL while the same concentration at 37 °C reduced FCV by 4.43 $\log_{10}$ TCID50/mL. In contrast, MNV-1 had only slight virus reductions (below 1 $\log_{10}$ TCID50/mL) even when the concentration of curcumin and the light dose was increased (50 μg/ml of CUR and 120 min of light irradiation) [51].

3.3.2. DNA viruses (enveloped and non-enveloped)

In general, from 26 studies with only *in vitro* activity, 16 included PDT in DNA viruses. From that, 14 were in enveloped DNA virus and 8 were in non-enveloped DNA virus. Moreover, the latter is represented by families *Adenoviridae* (represented by *Adenovirus* – AdV), *Parvoviridae* (Canine Parvovirus – CPV and Parvovirus B19), *Papillomaviridae* (Cottontail rabbit papillomavirus – CRPV), and *Polyomaviridae* (Mouse polyomavirus). The former is constituted by families *Baculoviridae* (Baculoviruses), *Herpesviridae* (Herpes simplex virus type 1 – HSV-1, Bovine herpesvirus type 1 – *BoHV-1*, Cytomegalovirus – CMV, Epstein–Barr Virus – EBV, Suid herpesvirus 1 – SHV-1, pseudorabies virus – PRV), and *Hepadnaviridae* (duck hepatitis B virus – DHVB and Hepatitis B virus – HBV) [61].

The most used PS was derived from porphyrin that was found in four studies for DNA viruses, as shown in Table 1 [45,48,54,55]. Latief et al. [45] investigated the PDT using porphyrin derivative TONS 504 against acyclovir (ACV)-sensitive and -resistant HSV-1 (enveloped DNA viruses). They found complete eradication of both strains at TONS 504 concentration of 10 mg/l and light energy of 10–30 J/cm^2, as well as, at 1 mg/l and light energy of 20 or 30 J/cm^2. Thus, this inactivation was effective depending on LED energy and PS concentration [45].

Lhotáková et al. [48] evaluated the PDT in two nanofibers materials:

polyurethane Tecophilic® and polycaprolactone (PCL), both containing 1 % of 5,10,15,20-tetraphenylporphyrin (TPP) as PS. Two DNA viruses were tested: a non-enveloped virus (mouse polyomavirus strain A2) and an enveloped DNA virus (recombinant baculovirus pVL-VP1). These nanofiber textiles were irradiated with white light for 30 min, and then, virus inactivation was evaluated through immunofluorescence. The viruses exposed to PDT were noninfectious for both nanofibers. They also demonstrated virus inactivation after 10 and 30 min of irradiation, showing that inhibition effects were similar for both textiles, but baculovirus was more resistant. In addition, they performed PDT using an analogue TPPS in aqueous solution incubated for 30 min. The concentration of TPPS above 0.0.5 % inhibited completely recombinant baculovirus pVL-VP1 and mouse polyomavirus. The concentration of 0.001 % TPPS resulted in a decrease of one order of magnitude in the infectivity of the mouse polyomavirus, while the baculovirus showed a more resistant profile, reducing its infectivity to approximately 65 %.

The photoinactivation using neutral and cationic tripyridylporphyrin-D-galactose conjugates were evaluated against HSV-1. It was observed that both compounds were effective singlet oxygen generators. Moreover, the neutral compound 1b was more efficient at the later times of the viral replication cycle assayed at 4 and 16 h post-infection, showing an inhibition of HSV-1 yield of 93.6 and 95.7 %, respectively. The cationic compound 3b highly inhibited the viral yield at all the addition times assayed, and similarly to compound 1b, the highest inhibition was also observed at the addition time 16 h post-adsorption with a reduction of 99.8 %. However, this compound 3b presented antiviral activity in the absence of light in all periods evaluated, while the neutral compound 1b displayed activity in the dark only in later time (16 h post-adsorption). Despite this, the photoactivation of these compounds seems to be necessary for their antiviral activity since a great reduction was achieved [54].

In addition to the tested RNA viruses as described above, the authors included an enveloped DNA virus PRV as model for hepatitis B virus, CMV and a non-enveloped DNA virus CPV as model for human parvovirus B19. When red cell concentrates (RCC) were inoculated with PRV and photoinactivated with Tri-P(4), a reduction of $\geq$ 4·6 $\log_{10}$ was achieved. In contrast, no reduction of virus titres was observed for CPV in all tested irradiation times [55]. Conjugates of phthalocyanines were applied as PS for DNA viruses in three *in vitro* studies [39,42,47] and one *in vivo* study [46].

Regarding the DNA virus, three oligolysine-conjugated phthalocyanines were investigated against *Adenovirus type 3* (Ad3) (non-enveloped) and HSV-1 (enveloped). They observed an inhibition against HSV-1, with half-maximal inhibitory concentration (IC_{50}) ranging from 0.05 to 0.46 for all PS used. However, they could not determine the IC_{50} values using concentrations up to 8 μM for these PS against Ad3 [42].

Lim et al. [47] included one non-enveloped DNA virus, Adenovirus type 5 (Ad5), for the PDT using near-infrared (NIR)-to-visible upconversion nanoparticles (UCNs) with ZnPc attached onto the surface. The best results were achieved using concentration of 440 μg/mL ZnPc-UCNs after exposure to NIR light (980 nm) at the light fluence of 14 kJ/cm^2. Only 18.66 % of the cells were infected, as compared to the control group that the infection affected 89.75 % of cells.

Photodynamic inactivation with ZnPc and AlPc as PS agents against the BoHV-1 enveloped DNA virus has been assessed [39]. This virus is associated with respiratory and reproductive infections in cattle that causes high economic loss. They observed a complete reduction of viral titers for both PS after irradiation (180 mW/cm^2) with a halogen lamp for 60 min. However, at concentration of 10 μM, a reduction of 4 logs in viral titer was detected for ZnPc after 15 min of irradiation that reached to zero after 30 min of irradiation.The cytopathic effect was not visualized. The increased efficiency of ZnPc was attributed to higher triplet quantum yields and higher singlet oxygen ($^1O_2$) production. Thus, ZnPc and AlPc mediated PDT are promising for photomedicine, and also could be applied against for other microorganisms of veterinary interest.

Only one paper applied PDT on non-enveloped DNA virus in an *in vivo* model [46] as presented in Table 2. In this study, skin grafts from the back of the ears of the New Zealand White rabbits were harvested and placed onto 7-mm wounds on the backs of CB-17 SCID mice. After 3 weeks, the epithelium was inoculated with CRPV. Cutaneous papillomas were growth by approximately 4 weeks (score 5). Then, 0.6 or 1.0 mg/kg of Pc 4 was administered intravenously *via* tail-vein for photoirradiation sessions with an interval of 48 h which consisted of a diode laser with 100 or 150 J/cm^2 and an irradiance of 75 mW/cm^2. The papillomas were measured every 7 days with a microcaliper millimeter and their volume was calculated. Tumor growth was reduced in the group treated with 1.0 mg/kg Pc 4 and 150 J/cm^2 laser light, resulting in complete regression in 13 tumors (87 %) from a total of 15 tumors treated [46].

Vigant et al. [33] also tested the LJ001 (rhodanine derivative) and JL103 (oxazolidine-2,4-dithione/ novel non-rhodanine compound) PS in enveloped DNA virus CMV and HSV-1 and in non-enveloped DNA virus Ad5. While the IC_{50} for CMV and HSV-1 were 147 nM and 20 nM for LJ001, respectively, the IC_{50} reduced to 5 nM for CMV and 2 nM for HSV-1 using JL103 which demonstrated better efficiency in generating $^1O_2$ than LJ001. In contrast, the PDT using LJ001 and JL103 did not show any effect for Ad5. Information about fluence and fluence rate were not informed. In addition, they generated a series of active oxazolidine-2,4-dithiones compounds (JL118 and JL122) that were efficient in generating $^1O_2$, but maintained antiviral activity at physiological hematocrits. When tested against HSV-1, the IC_{50} was 10.1 nM for JL118 and 2.4 nM for JL122.Thus, these compounds have demonstrated to inactivate the virus effectively, with improved properties relating to $^1O_2$ quantum yields and red-shifted absorption spectra.

The amotosalen as PS was investigated in two articles [52,53]. Singh et al. [53] included enveloped DNA viruses such as HBV and DHBV and a non-enveloped DNA virus: *Human adenovirus 5* (HAdV-5). They obtained effective inactivation in all these viruses, with reductions greater than 4 $\log_{10}$ [53]. In the other study, human platelet concentrates (PLT) were infected with non-enveloped DNA virus parvovirus B19, and then, submitted to photochemical treatment with 150 μmol/L of amotosalen-HCl for 5−90 min and UVA light at fluence of 3.0 J/cm^2. The preincubation of 60, 75, and 90 min before photoinactivation resulted in reductions of 5.3 $\log_{10}$, 5.6 $\log_{10}$, and 5.8 $\log_{10}$ of parvovirus B19 infectivity in PLTs, respectively. Thus, these results demonstrated that PCT with amotosalen-HCl and UVA irradiation was effective in eliminating the refractory virus parvovirus B19 in a blood product [52].

The study of PDT mediated by Zn-BC-AM was investigated in the nasopharyngeal carcinoma (NPC) that has been associated with enveloped DNA virus EBV infection. Zn-BC-AM-PDT induced death of HK-1-EBV cells in 50 % when irradiation dose was 0.5 J/cm^2 and 80 % at 1 J/cm^2. In addition, the PDT increased cytokine production of IL-1 and IL-6 and suppression of IL-8, suggesting a role in the modulation of immune response. They also suggested, based on these results, further application of Zn-BC-AM PDT for the treatment of NPC [43].

Mohr et al. [49] also included an enveloped DNA virus SHV-1, for PDT in FFP using MB and monochromatic yellow light as described above for RNA virus. A complete eradication exceeding a reduction of 5.71 $\log_{10}$ was achieved using MB concentration of 0.8 μmol/L and a light dose of 150–200 J/cm^2. However, SHV-1 was relatively resistant, as a higher light dose was necessary to inactivate the virus when compared to RNA virus HIV-1 that needed 20−40 J/cm^2 to be eradicated.

ALA-PDT against the DNA enveloped virus HSV-1 at 0.05 and 0.1 mM concentrations and irradiated with a tungsten lamp were tested. The post-adsorption assay treatment, HaCat cells were first incubated with HSV-1, and then ALA was added and photoirradiated. The results show a concentration-dependent inhibition of HSV-1 replication about 40 % for ALA 0.05 mM and 70 % for ALA 0.1 mM. They suggest that ALA-PDT acts directly in a late phase of the viral cycle, interfering the formation of the new viral particles and limiting the virus spread [36].

Monjo et al. [32] also evaluated the photodynamic inactivation (PDI)

of Orthoquin against three DNA viruses: two enveloped (HSV-1 and HSV-2) (and one non-enveloped (AdV5). The irradiation was performed with 65 W LED light for 10 min (12.6 J/cm^2, 21 mW/cm^2) for HSV-1 and AdV, and for 5 min for HSV-1 since it is photosentive. Orthoquin-PDT resulted in a reduction in plaque formation at 0.05 and 0.1 μg/mL for HSV-1 and at 0.1 μg/mL for HSV-2, in a light-dependent manner. In contrast, in an independent light-manner, high concentrations (0.5 and 1.0 μg/mL) from PS were able to triggera significant reduction of PFU for HSV-1 and HSV-2 Ortoquin-PDT (0.5 and 1 μg/mL) was able to significatively reduce AdV plaque, in a light-dependent condition. They also demonstrated that only when Ortoquin and light were co-administered with HSV-1 was effective in inactivating virus, while pre-exposure of Orthoquin to light did not reduce plaque formation. It indicates that Ortoquin needs direct contact with target virions during light exposure. The inactivation on HSV-1 may be due to physical damage to proteins present on the virion exterior, which in turn will prevent infection [32].

The effect of ICG-PDT was analyzed with two infra-red diode lasers with 810 and 940 nm wavelength against the HSV-1enveloped DNA. ICG irradiated with 810 and 940 nm diode laser reduced significantly the count of HSV1/mL to 1.548×10^5 and to 2.484×10^5, respectively, in comparison to control (9.0×10^5). Moreover, the reduction was significantly higher when irradiated with 810 nm laser than with 940 nm laser [50].

Zverev et al. [60] using fotoditazine against enveloped DNA HSV-1 found a reduction in viral titer of 1000-fold or greater (1.5–2.5 orders of magnitude) in doses of 50 μg/mL or higher. However, concentrations of 50 and 100 μg/mL of the PS were cytotoxic for Vero cells as indicated by cell degradation [60].

3.4. Evaluation risk of bias

The risk of bias was analyzed for 26 selected publications available in Fig. 2. The score of 26 publications (24 exclusively *in vitro* and two with *in vitro/ in vivo* part) varied from 4 to 10 among 15 domains established by the checklist. The trials exclusively *in vitro* or with a part *in vitro* [33, 36–60] presented between 80–100% the domains for low risk of bias (structured abstract, scientific background and rationale, objectives and/or hypotheses, the intervention of each group, outcomes, sample size, statistical methods, and funding). On the other hand, these publications pointed to a high risk of bias domains (randomization - sequence generation, allocation concealment mechanism, implementation, blinding, limitations, and protocol) have not been reported in 92–100% of studies *in vitro* or with a part *in vitro*. Fig. 3 highlights one assay exclusively *in vivo* [46] and two with an *in vivo / in vitro* part [47,57] with a score ranging from 4 to 6 of the ten domains of the checklist. For *in vivo* studies, five domains for low risk of bias (allocation sequence generation, baseline characteristics, allocation concealment, random Housing, and other sources of bias) were reported in 67–100% of *in vivo* trials. Similarly, five domains for high risk of bias (blinding of personnel & participants, random outcome assessment, outcome assessor blinding, incomplete outcome data, and selective outcome reporting) were not reported in 67–100% of *in vivo* trials. No publication selected in the systematic review presented all domains for identifying the risk of bias.

4. Discussion

This review provides a systematic search of literature between 2004 and 2020 for PDT effect on RNA and DNA enveloped and non-enveloped viruses. Many topical treatments for virus diseases have been investigated, however this review highlights 27 studies and includes photodynamic treatments that used many PS and light sources to viral photoinactivation. Our findings reveal PDT as a potential alternative therapy, mainly when the immunization through vaccines is not yet available or even conventional drugs fail to treat diseases caused by viruses in humans.

The morphology of the new coronavirus has already been elucidated and the pathophysiology of this disease is being studied [5,6] meanwhile, a vaccine or efficient drug directed to the treatment of COVID-19 is not yet available. The focus of the present systematic review was designed to address the following question: “Could photodynamic therapy have an effect on COVID-19?”. In this study it is assumed that PDT would also have an effect on SARS-CoV-2, for several reasons. First, SARS-CoV-2 is an enveloped RNA virus, and in this review 26 *in vitro* studies used PDT with a variety of PS pointed to significant reductions to viral inactivation in enveloped and non-enveloped RNA viruses, as shown in Table 1. Several studies that used PDT mediated by different types of photosensitizers in order to inactivate both DNA and RNA viruses, reported that this technique can destroy the integrity of genetic material as well as viral structures, such as capsid proteins and envelope lipids, are usually the main targets to destruction from PDT, the

Study *in vitro*	Checklist item															
	1	2a	2b	3	4	5	6	7	8	9	10	11	12	13	14	15
Huang et al 2004	+	+	+	-	-	?	-	-	-	-	-	-	-	+	-	4
Mohr et al 2004	+	+	+	+	?	?	-	-	-	-	-	-	-	-	-	4
Trannoy et al 2016	+	+	+	+	+	+	-	-	-	-	+	-	-	-	-	7
Singh et al 2006	+	+	+	+	?	+	-	-	-	-	+	-	-	+	-	7
Tome´ et al 2007	-	+	+	+	-	+	-	-	-	-	+	?	?	+	-	6
Sawyer et al 2007	+	+	+	+	+	+	-	-	-	-	+	?	-	+	-	8
Vargas et al 2008	-	+	+	+	+	+	-	-	-	-	+	+	-	-	-	7
Ayala et al 2008	+	+	+	+	+	+	-	-	-	-	+	?	-	-	-	7
Belanger et al 2010	+	+	+	+	+	+	-	-	-	-	+	-	-	+	-	8
Koon et al 2010	+	+	+	+	+	+	-	-	-	-	+	-	-	+	-	8
Lhotáková et al 2012	-	+	+	+	+	+	-	-	-	-	-	?	-	+	-	5
Ke et al 2014	+	+	+	+	+	+	-	-	-	-	+	?	-	+	-	8
Belousova et al 2014	+	+	+	+	+	+	-	-	-	-	+	+	-	-	-	7
Cruz-Oliveira et al 2017	+	+	+	+	+	-	-	-	-	-	+	-	?	+	-	7
Latief et al 2015	+	+	+	+	+	+	-	-	-	-	+	-	?	+	-	9
Randazzo et al 2016	+	+	+	+	+	+	-	-	-	-	+	+	-	+	-	9
Zverev et al 2016	+	+	+	+	+	+	-	-	-	-	+	-	-	+	-	8
Cocca et al 2017	+	+	+	+	+	-	-	-	-	-	+	+	-	+	-	8
Korneev et al 2019	+	+	+	+	+	+	-	-	-	-	-	-	-	+	-	7
Xu et al 2019	+	+	+	+	+	+	-	-	-	-	+	+	-	+	-	9
Namvar et al 2019	+	+	+	+	+	+	-	-	-	-	+	+	-	+	-	9
Yin et al 2012	+	+	+	+	+	+	-	-	-	-	+	+	-	+	-	8
Vigant et al 2013	+	+	+	+	+	+	-	-	-	-	+	+	+	+	-	7
Study *in vitro**																
Lim et al 2012	-	+	+	+	+	-	-	-	-	-	+	-	-	+	-	6
Wu et al 2015	+	+	+	+	+	+	?	-	-	-	+	-	-	+	-	8

Fig. 2. Risk of bias of *in vitro* studies' according to the modified CONSORT checklist. *In two trial both methods (*in vitro* and *in vitro* studies) were investigated. *Part A (*in vitro* studies). 1) Structured abstract; 2a) Scientific background and rationale; 2b) Objectives and/or hypotheses; 3) Intervention of each group; 4) Outcomes; 5) Sample size; 6) Randomization: sequence generation; 7) Allocation concealment mechanism; 8) Implementation; 9) Blinding; 10) Statistical methods; 11) Outcomes and estimation; 12) Limitations; 13) Funding; 14) Protocol; 15) Scores. (+) Low risk of bias; (-) High risk of bias; (?) Unclear risk of bias. *.

Study *in vivo*	Checklist item										
	1	2	3	4	5	6	7	8	9	10	11
Lim et al 2012*	-	+	+	+	-	-	-	-	-	+	4
Wu et al 2015*	+	+	+	+	-	-	-	+	-	-	5
Lee et al 2010**	+	+	+	+	-	-	-	-	+	+	6

Fig. 3. Assessment of the risk of bias *in vivo* studies at an individual level, according to SYRCLE's ROB tool. *In two trial both methods (*in vitro* and *in vitro* studies) were investigated. *Part B (*in vivo* studies). **exclusively *in vivo* trial. Allocation sequence generation; 2) Baseline characteristics; 3) Allocation concealment; 4) Random Housing; 5) Blinding of personnel & participants; 6) Random outcome assessment; 7) Outcome assessor blinding; 8) Incomplete outcome data; 9) Selective outcome reporting; 10) Other sources of bias; 11) Scores. Low risk of bias; High risk of bias; Unclear risk of bias. *.

photoinactivation external structures promotes the extravasation of viral content inactivating viral enzymes [36,42,57,62]. Besides that, the PDT was able to detach from surface glycoproteins viral, hence completely inactivating an enveloped RNA virus (H5N8), that belongs to class similarly with SARS-CoV-2 [44].

Furthermore, studies with photoinactivation using human material *in vitro* such as red cells concentrates [55], human platelet concentrates [52] and in fresh frozen plasma [49,53] presented inactivations of RNA virus and DNA, but mainly for the enveloped RNA virus the reductions were almost at 100 % for viral titles. Singh et al. [53] evaluated the effect of Amotosalen with UVA and showed effectiveness in the treatment of plasma infected with different types of viruses, especially for the SARS-CoV virus which obtained almost complete photoinactivation. Considering that SARS-CoV and SARS-CoV-2 belong to *Coronaviridae* family and cause severe acute respiratory syndrome coronavirus in humans, and the similarity in both viruses to use the ACE2 as a receptor to infect ciliated bronchial epithelial cells [63,64], since the action of PDT on plasma infected with SARS-CoV has been reported [53], its use to treat patients with the novel severe acute respiratory syndrome coronavirus 2 in severe stages could be an alternative approach.

The PDT was efficient also in *in vivo* studies, shown in Table 2, as the use of ZnPc-UCNs-PDT on model infected mice with DENV2 [47], and derivatives of oxazolidine-2,4-dithiones mediated by PDT showed an antiviral efficacy against a RVFV [33]. These arboviruses that affect humans, and belong to the class of enveloped RNA viruses like the new coronavirus. Although these studies use different methodologies to compose the PDT, all of them showed success of photoinactivation of enveloped RNA viruses, suggesting that it could be an effective approach to SARS-CoV-2 inactivation.

The effectiveness of a wide range of PS together with various light sources used in PDT, showed effective action in this review on most DNA and RNA viruses with envelope or not. However, some studies have pointed out some resistance to non-enveloped DNA viruses, such as Adv and CPV [33,42,55] and non-enveloped RNA viruses, such as MNV-1 and Cox Virus [42,51]. In generally, the low efficiency of PDT reported for these viruses may be related to several factors, from the type of PS used, the concentration used, the pre-incubation time, may also be related to the light source, dose, illumination distance and time [32,38,39,41,42,45,48,49,54,55] even to the virulence capacity or resistance of these viruses such as non-enveloped virus DNA or RNA [33,42,55], which may have low affinity with the PS and light sources tested.

In addition, PDT can also be used in the first stage for the production of vaccine, which uses the genetic material of the inactivated virus, being considered an effective and faster method according to Ayala et al. [36] and Belanger et al. [37].

Nevertheless, in all studies that evaluated the effect of photoinactivation on enveloped RNA viruses, PDT was successful, regardless of the PS or light source used. The results of these articles direct us strongly to understand that this methodology could be implemented to photoactivated SARS-CoV-2, consequently assisting in the treatment of COVID-19.

5. Strengths and limitations of the study

The systematic review was through several phases, and used five databases and Google Scholar system to provide a precision robust, stable and comprehensive metric way in the search for publications. The identification and choice of MesH terms was cautious, as well as the eligibility criteria of the selected articles which were decided by several researchers by consensus, providing high sensitivity and specificity. The studies with *in vitro* and *in vivo* methodology selected, covers multiple protocols, with different PS and concentrations, light type, duration of photoinactivation and different methods of quantitative analysis. A limitation of this study was the selection of publications only in the English language. The broad variability among these protocols resulted in a low standard uniform to quantitative analysis observed in the articles selected, leading it impossible to compare the studies directly due to heterogeneity and meta-analysis.

The analysis of the risk of bias highlights that many studies fail or do not value the complete description of the checklist domains to assess methodological quality. The absence of many essential domains (randomization, allocation concealment mechanism, blinding, incomplete outcome data, selective outcome reporting, limitations, and protocol) allows the identification of high risk of bias or unclear bias in publications. The notable absence of domains to identify the risk of bias in publications included in this systematic review shows a relevant limitation. Among the experimental studies *in vitro* as *in vivo*, only one study of each method presented 10 out of 15 domains [32] and 6 out of 10 [46] domains of the checklists, respectively. In addition, information about one *in vivo* experiment was not included in this review due to miss information in the article and failure to obtain a response from the authors. It is suggested to the researchers, in general, a more significant observance regarding the domains provided by the checklists for identification of risk bias, mainly in experimental tests.

6. Conclusion

The available evidence summarized in this review supports the use of PDT could be applied to photoactivated the enveloped RNA virus SARS-CoV-2. In view of this, we can cautiously infer that PDT could be a potentially effective and safe treatment for COVID-19 in the future. However, due to the high heterogeneity of the protocols, we observed an immense range of different PS and light sources used, we recommend that these data may serve as support for future trials in the new coronavirus, since the literature is still unknown about the use of PDT for SARS-CoV-2.

Funding

The authors thank the National Council of Technological and Scientific Development Foundation (CNPq), and Technology and Higher Education Foundation (CAPES) for the support received (scholarship).

Declaration of Competing Interest

The authors report no declarations of interest.

Acknowledgement

Thanks for the dedication and contribution of each author to this review.

Appendix A. Supplementary data

Supplementary material related to this article can be found, in the online version, at doi:https://doi.org/10.1016/j.pdpdt.2021.102221.

References

[1] Coronavirus Disease (COVID-19) - Situation Report- 161, World Health Organization, 2020 (Accessed 16 December 2020), https://www.who.int/docs/default-source/coronaviruse/situation-reports/20200629-covid-19-sitrep-161.pdf?sfvrsn=74fde64e_2.
[2] N. Zhu, et al., A Novel Coronavirus from Patients with Pneumonia in China, 2019, N. Engl. J. Med. 382 (8) (2020) 727–733, https://doi.org/10.1016/j.cell.2020.04.011.
[3] V.M. Corman, et al., Hosts and sources of endemic human coronaviruses, Adv. Virus Res. 100 (2018) 163–188, https://doi.org/10.1016/bs.aivir.2018.01.001.
[4] J. Liu, et al., Overlapping and discrete aspects of the pathology and pathogenesis of the emerging human pathogenic coronaviruses SARS-CoV, MERS-CoV, and 2019-nCoV, J. Med. Virol. 92 (5) (2020) 491–494, https://doi.org/10.1002/jmv.25709.
[5] D. Kim, et al., The architecture of SARS-CoV-2 transcriptome, Cell 181 (2020) 1–8, https://doi.org/10.1016/j.cell.2020.04.011.
[6] M. Cevik, et al., Virology, transmission, and pathogenesis of SARS-CoV-2, BMJ 23 (2020), https://doi.org/10.1136/bmj.m3862.
[7] R. Yan, et al., Structural basis for the recognition of SARS-CoV-2 by full-length human ACE2, Science 367 (6485) (2020) 1444–1448, https://doi.org/10.1126/science.abb2762.
[8] J. Shang, et al., Structural basis of receptor recognition by SARS-CoV-2, Nature 581 (7807) (2020) 221–224, https://doi.org/10.1038/s41586-020-2179-y.
[9] A. Wu, et al., Genome composition and divergence of the novel coronavirus (2019-nCoV) originating in China, Cell Host Microbe 27 (3) (2020) 325–328, https://doi.org/10.1016/j.chom.2020.02.001.
[10] W. Liu, et al., COVID-19: Attacks the 1-Beta Chain of Hemoglobin and Captures the Porphyrin to Inhibit Heme Metabolism, ChemRxiv, 2020, pp. 1–38, https://doi.org/10.26434/chemrxiv.11938173.
[11] H.K. Siddiqi, et al., COVID-19 illness in native and immunosuppressed states: a clinical-therapeutic staging proposal, J. Heart Lung Transplant. 39 (5) (2020) 405–407, https://doi.org/10.1016/j.healun.2020.03.012.
[12] K.G. Andersen, et al., The proximal origin of SARS-CoV-2, Nat. Med. 26 (4) (2020) 450–452, https://doi.org/10.1038/s41591-020-0820-9.
[13] C.P. Sabino, et al., Global priority multidrug-resistant pathogens do not resist photodynamic therapy, J. Photochem. Photobiol. B (2020) 1–41, https://doi.org/10.1016/j.jphotobiol.2020.111893.
[14] K.M. Sakita, et al., Copolymeric micelles as efficient inert nanocarrier for hypericin in the photodynamic inactivation of Candida species, Future Microbiol. 14 (2019) 519–531, https://doi.org/10.2217/fmb-2018-0304.
[15] C.B. Galinari, et al., Nanoencapsulated hypericin in P-123 associated with photodynamic therapy for the treatment of dermatophytosis, J. Photochem. Photobiol. B 215 (2021) 112103, https://doi.org/10.1016/j.jphotobiol.2020.112103.
[16] S. Khan, et al., Inhibition of multi-drug resistant Klebsiella pneumoniae: nanoparticles induced photoinactivation in presence of efflux pump inhibitor, Eur. J. Pharm. Biopharm. 157 (2020) 165–174, https://doi.org/10.1016/j.ejpb.2020.10.007.
[17] O. Gulías, et al., Effective photodynamic inactivation of 26 Escherichia coli strains with different antibiotic susceptibility profiles: a planktonic and biofilm study, Antibiotics 9 (3) (2020) 1–12, https://doi.org/10.3390/antibiotics9030098.
[18] F.A.P. de Morais, et al., Hypericin photodynamic activity. Part III: in vitro evaluation in different nanocarriers against trypomastigotes of Trypanosoma cruzi, Photochem. Photobiol. Sci. 18 (2) (2019) 487–494, https://doi.org/10.1039/c8pp00444g.
[19] A.F.S. Barbosa, et al., Anti-Trypanosoma cruzi effect of the photodynamic antiparasitic chemotherapy using phenothiazine derivatives as photosensitizers, Lasers Med. Sci. 35 (1) (2020) 79–85, https://doi.org/10.1007/s10103-019-02795-4.
[20] A.L. Selva, et al., Treatment of herpes labialis by photodynamic therapy: study protocol clinical trial (SPIRIT compliant), Medicine 99 (12) (2020) 1–9, https://doi.org/10.1097/MD.0000000000019500.
[21] E.M. Alvarado, et al., Effectiveness of photodynamic therapy in elimination of HPV-16 and HPV-18 associated with CIN I in mexican women, Photochem. Photobiol. 93 (5) (2017) 1269–1275, https://doi.org/10.1111/php.12769.
[22] J. Wang, et al., Human papillomavirus DNA detection-guided ALA-photodynamic therapy for anogenital condyloma acuminata: a report of two cases, Photodiagnosis Photodyn. Ther. 25 (2019) 460–462, https://doi.org/10.1016/j.pdpdt.2019.02.003.
[23] L.F. Morgado, et al., Photodynamic Therapy treatment of onychomycosis with Aluminium-Phthalocyanine Chloride nanoemulsions: a proof of concept clinical trial, J. Photochem. Photobiol. B 173 (2017) 266–270, https://doi.org/10.1016/j.jphotobiol.2017.06.010.
[24] F.P. Eduardo, et al., Severe oral infection caused by Pseudomonas aeruginosa effectively treated with methylene blue-mediated photodynamic inactivation, Photodiagn Photodyn Ther (2019) 284–286, https://doi.org/10.1016/j.pdpdt.2019.04.013.
[25] H.H. Buzzá, et al., Overall results for a national program of photodynamic therapy for basal cell carcinoma: a multicenter clinical study to bring new techniques to social health care, Cancer Control 26 (2019) 1–12, https://doi.org/10.1177/1073274819856885.
[26] M.B. Johansen, et al., Effective treatment with photodynamic therapy of cutaneous leishmaniasis: a case report, Dermatol. Ther. 32 (5) (2019) 1–12, https://doi.org/10.1111/dth.13022.
[27] B. Knyazer, et al., Accelerated corneal cross-linking with photoactivated chromophore for moderate therapy-resistant infectious keratitis, Cornea 37 (4) (2018) 528–531, https://doi.org/10.1097/ICO.0000000000001498.
[28] C. Fisher, et al., Photodynamic therapy for the treatment of vertebral metastases: a phase I clinical trial, Clin. Cancer Res. 25 (19) (2019) 5766–5776, https://doi.org/10.1158/1078-0432.CCR-19-0673.
[29] J.M. DeWitt, et al., Phase 1 study of EUS-guided photodynamic therapy for locally advanced pancreatic cancer, Gastrointest. Endosc. 89 (2) (2019) 390–398, https://doi.org/10.1016/j.gie.2018.09.007.
[30] A.P. Castano, et al., Mechanisms in photodynamic therapy: part two-cellular signaling, cell metabolism and modes of cell death, Photodiagn Photodyn Ther 2 (1) (2005) 1–23, https://doi.org/10.1016/S1572-1000(05)00030-X.
[31] A. Wiehe, et al., Trends and targets in antiviral phototherapy, Photochem. Photobiol. Sci. 18 (11) (2019) 2565–2612, https://doi.org/10.1039/c9pp00211a.
[32] A.L.A. Monjo, et al., Photodynamic inactivation of herpes simplex viruses, Viruses 10 (10) (2018) 1–16, https://doi.org/10.3390/v10100532.
[33] F. Vigant, et al., A mechanistic paradigm for broad-spectrum antivirals that target virus-cell fusion, PLoS Pathog. 9 (4) (2013) 1–15, https://doi.org/10.1371/journal.ppat.1003297.
[34] C.M. Faggion Jr, Guidelines for reporting pre-clinical in vitro studies on dental materials, J. Evid. Dent. Pract. 12 (4) (2012) 182–189, https://doi.org/10.1016/j.jebdp.2012.10.001.
[35] C.R. Hooijmans, et al., SYRCLE's risk of bias tool for animal studies, BMC Med. Res. Methodol. 14 (43) (2014) 1–9, https://doi.org/10.1186/1471-2288-14-43.
[36] F. Ayala, et al., 5-aminolaevulinic acid and photodynamic therapy reduce HSV-1 replication in HaCat cells through an apoptosis-independent mechanism, Photodermatol. Photoimmunol. Photomed. 24 (5) (2008) 237–243, https://doi.org/10.1111/j.1600-0781.2008.00367.x.
[37] J.M. Belanger, et al., Characterization of the effects of aryl-azido compounds and UVA irradiation on the viral proteins and infectivity of human immunodeficiency virus type 1, Photochem. Photobiol. 86 (5) (2010) 1099–1108, https://doi.org/10.1111/j.1751-1097.2010.00780.x.
[38] I.M. Belousova, et al., Photodynamic inactivation of enveloped virus in protein plasma preparations by solid-phase fullerene-based photosensitizer, Photodiag. Photodyn. Ther. 11 (2) (2014) 165–170, https://doi.org/10.1016/j.pdpdt.2014.02.009.
[39] L.H.Z. Cocca, et al., Tetracarboxy-phthalocyanines: from excited state dynamics to photodynamic inactivation against Bovine herpesvirus type 1, J. Photochem. Photobiol. B 175 (2017) 1–8, https://doi.org/10.1016/j.jphotobiol.2017.08.019.
[40] C. Cruz-Oliveira, et al., Mechanisms of vesicular stomatitis virus inactivation by protoporphyrin IX, zinc-protoporphyrin IX, and mesoporphyrin IX, Antimicrob. Agents Chemother. 61 (6) (2017) 1–36, https://doi.org/10.1128/AAC.00053-17.
[41] Q. Huang, et al., Inactivation of dengue virus by methylene blue/narrow bandwidth light system, J. Photochem. Photobiol. B Biol. 77 (1–3) (2004) 39–43, https://doi.org/10.1016/j.jphotobiol.2004.08.005.
[42] M.R. Ke, et al., Oligolysine-conjugated zinc (II) phthalocyanines as efficient photosensitizers for antimicrobial photodynamic therapy, Chem. Asian J. 9 (7) (2014) 1868–1875, https://doi.org/10.1002/asia.201402025.
[43] H.K. Koon, et al., Photodynamic therapy-mediated modulation of inflammatory cytokine production by Epstein-Barr virus-infected nasopharyngeal carcinoma cells, Cell. Mol. Immunol. 7 (4) (2010) 323–326, https://doi.org/10.1038/cmi.2010.4.
[44] D. Korneev, et al., Ultrastructural aspects of photodynamic inactivation of highly pathogenic avian H5N8 influenza virus, Viruses 11 (10) (2019) 1–11, https://doi.org/10.3390/v11100955.
[45] M.A. Latief, et al., Inactivation of acyclovir-sensitive and -resistant strains of herpes simplex virus type 1 in vitro by photodynamic antimicrobial chemotherapy, Mol. Vis. 21 (2015) 532–537.
[46] R.G. Lee, et al., Photodynamic therapy of cottontail rabbit papillomavirus-induced papillomas in a severe combined immunodeficient mouse xenograft system, Laryngoscope 120 (3) (2010) 618–624, https://doi.org/10.1002/lary.20709.
[47] M.E. Lim, et al., Photodynamic inactivation of viruses using upconversion nanoparticles, Biomaterials 33 (6) (2012) 1912–1920, https://doi.org/10.1016/j.biomaterials.2011.11.033.
[48] Y. Lhotáková, et al., Virucidal nanofiber textiles based on photosensitized production of singlet oxygen, PLoS One 7 (11) (2012) 1–9, https://doi.org/10.1371/journal.pone.0049226.
[49] H. Mohr, et al., West Nile virus in plasma is highly sensitive to methylene blue-light treatment, Transfusion 44 (6) (2004) 886–890, https://doi.org/10.1371/journal.pone.0049226.
[50] M.A. Namvar, et al., Effect of photodynamic therapy by 810 and 940 nm diode laser on Herpes Simplex Virus 1: an in vitro study, Photodiagn. Photodyn. Ther. 25 (2019) 87–91, https://doi.org/10.1016/j.pdpdt.2018.11.011.

[51] W. Randazzo, et al., Curcumin-mediated photodynamic inactivation of norovirus surrogates, Food Environ. Virol. 8 (4) (2016) 244–250, https://doi.org/10.1007/s12560-016-9255-3.
[52] L. Sawyer, et al., Inactivation of parvovirus B19 in human platelet concentrates by treatment with amotosalen and ultraviolet A illumination, Transfusion 47 (6) (2007) 1062–1070, https://doi.org/10.1111/j.1537-2995.2007.01237.x.
[53] Y. Singh, et al., Photochemical treatment of plasma with amotosalen and long-wavelength ultraviolet light inactivates pathogens while retaining coagulation function, Transfusion 46 (7) (2006) 1168–1177, https://doi.org/10.1111/j.1537-2995.2006.00867.x.
[54] J.P.C. Tomé, et al., Synthesis of neutral and cationic tripyridylporphyrin-D-galactose conjugates and the photoinactivation of HSV-1, Bioorg. Med. Chem. 15 (14) (2007) 4705–4713, https://doi.org/10.1016/j.bmc.2007.05.005.
[55] L.L. Trannoy, et al., Differential sensitivities of pathogens in red cell concentrates to Tri-P(4)-photoinactivation, Vox Sang. 91 (2) (2006) 111–118, https://doi.org/10.1111/j.1423-0410.2006.00791.x.
[56] F. Vargas, et al., Comparative antiviral (HIV) photoactivity of metalized meso-tetraphenylsulfonated porphyrins, Med. Chem. 4 (2) (2008) 138–145, https://doi.org/10.2174/157340608783789167.
[57] J. Wu, et al., Virucidal efficacy of treatment with photodynamically activated curcumin on murine norovirus bio-accumulated in oysters, Photodiagn. Photodyn. Ther. 12 (3) (2015) 385–392, https://doi.org/10.1016/j.pdpdt.2015.06.005.
[58] L. Xu, et al., Hypericin-photodynamic therapy inhibits the growth of adult T-cell leukemia cells through induction of apoptosis and suppression of viral transcription, Retrovirology 16 (5) (2019) 1–13, https://doi.org/10.1186/s12977-019-0467-0.
[59] H. Yin, et al., Photoinactivation of cell-free human immunodeficiency virus by hematoporphyrin monomethyl ether, Lasers Med. Sci. 27 (5) (2012) 943–950, https://doi.org/10.1007/s10103-011-1013-z.
[60] V.V. Zverev, et al., In vitro studies of the antiherpetic effect of photodynamic therapy, Lasers Med. Sci. 31 (5) (2016) 849–855, https://doi.org/10.1007/s10103-016-1912-0.
[61] P.T. Ho, et al., VIPERbd: a tool for virus research, Ann. Rev. 5 (2018) 477–488, https://doi.org/10.1146/annurev-virology-092917-043405.
[62] L. Costa, et al., Evaluation of resistance development and viability recovery by a non-enveloped virus after repeated cycles of aPDT, Antiviral Res. 91 (2011) 278–282, https://doi.org/10.1016/j.antiviral.2011.06.007.
[63] W. Li, et al., Angiotensin-converting enzyme 2 is a functional receptor for the SARS coronavirus, Nature 426 (6965) (2003) 450–454, https://doi.org/10.1038/nature02145.
[64] M. Hussain, et al., Structural variations in human ACE2 may influence its binding with SARS-CoV-2 spike protein, J. Med. Virol. 92 (9) (2020) 1580–1586, https://doi.org/10.1002/jmv.25832.